Power Quality Assessment of Electric Distribution Grids Integrated with Distributed Energy Resources

Jens William Foyer, Mariusz Maruszak

Energy Technology, EPSH4-1033, 2020-05

Master Thesis

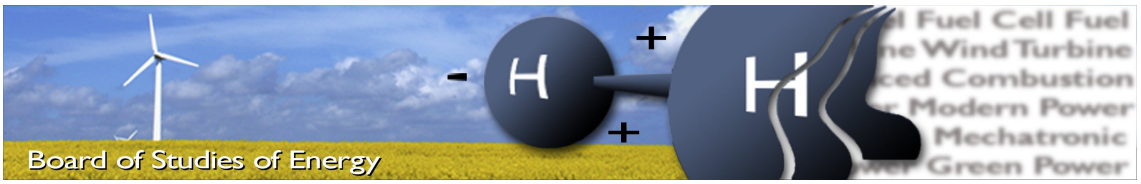

Title:	Power Quality Assessment of Electric Distribution Grids Integrated with Distributed Energy Sources
Semester:	4
Semester theme:	Master thesis
Project period:	03.02.20 to 29.05.20
ECTS:	30
Supervisor:	Sanjay Chaudhary
Project group:	EPSH4-1033

Jens Foyer

Mariusz Maruszak

SYNOPSIS:

Power systems are changing from centralized systems with big conventional power plants to distributed systems with renewable energy sources. Along with that, more power quality problems appear in the grid. This project focuses on harmonic studies for a single low-voltage feeder with photovoltaics and battery storage. The system is considered to be balanced with two types of converters: three-phase Graetz bridge and 2-level voltage source converter. Individual impact of a converter on the grid is investigated with di□erent power ratings. Moreover the combination of two di□erent converters connected at the same time to the grid is performed. The study is carried out in Powerfactory simulation software.

Pages, total:	55
Appendix:	1
Supplements:	0

By accepting the request from the fellow student who uploads the study group's project report in Digital Exam System, you confirm that all group members have participated in the project work, and thereby all members are collectively liable for the contents of the report. Furthermore, all group members confirm that the report does not include plagiarism.

Summary

The trend of increased nonlinear devices such a renewable energy sources and switched-mode power supplies in the modern electric grid has made significant changes to power flow and quality. Power sources such as grid-tied photovoltaic (PV) systems combined with a battery have the potential to shift where most of a home's electricity comes from. The main loads analyzed are photovoltaic inverters and electric vehicle (EV) chargers. Since these nonlinear loads can output harmful distortions into the grid, it's important to understand how they operate.

This study focuses on how the amount of nonlinear loads a□ects harmonic power quality. Solutions to reduce harmonic distortion in the feeder are also explored. A distribution grid based on a CIGRE benchmark grid for renewable energy studies is used for the simulations. Background harmonics from the medium-voltage grid are considered. First, an assumption of PV harmonic injections is made based on the characteristic harmonics and the standard limits to observe how they a□ect the grid. Later, a method for determining the equivalent model of a PV inverter is used to analyze the harmonic currents absorbed from the grid. The EV charger characteristic harmonics are analyzed to compare unfiltered and filtered variants. The study case results are compared to relevant power quality standards for validation. The e□ect of resonance from the added loads is analyzed. An estimation of the maximum PV penetration is made based on the power quality limits.

Harmonic filtering is used as a key method of reducing harmonic distortion in this study. Single-tuned and damped filters are designed to mitigate the harmonics from the electric vehicle chargers as well as reduce the grid distortions from other sources. E□ects of filtering on the resonant frequencies in the grid are studied.

Nomenclature List

Special Symbols and Denotations

Symbol	Description	Derived unit	Unit
B	Susceptance	Siemens	S
C	Capacitance	Farad	F
f	Frequency	Hertz	Hz
G	Conductance	Siemens	S
I	Current	Ampere	A
L	Inductance	Henry	H
P	Active power	Watt	W
p	Number of pulses	-	-
R	Resistance	Ohm	Ω
S	Apparent power	Volt-ampere	VA
t	Time	Seconds	s
U	Voltage	Volt	V
X	Reactance	Ohm	Ω
Y	Admittance	Siemens	S
Z	Impedance	Ohm	Ω
Q	Reactive power	Volt-ampere-reactive	VAR
QF	Quality Factor	-	-
δ	Relative frequency deviation	-	-
θ	Phase angle	Degrees	$^\circ$
ρ	Power factor	-	-
ρ_f	Filter e□ectiveness	-	-
ϕ	Phase di□erence	Degrees	$^\circ$
ω	Angular frequency	radians per seconds	rad/s
ω_n	Resonance frequency	Hertz	Hz

Acronyms

Acronym	Abbreviation of:
DER	Distributed Energy Sources
DSO	Distribution System Operator
EV	Electric Vehicle
IEC	International Electrotechnical Commission
IEEE	Institute of Electrical and Electronics Engineers
LV	Low Voltage
MV	Medium Voltage
PCC	Point of Common Coupling
PHEV	Plug - in Hybrid Electric Vehicles
PLL	Phase Locked Loop
PWM	Pulse Width Modulation
PV	Photovoltaic
RES	Renewable Energy Source
RMS	Root mean square
SCR	Short - Circuit Ratio
TDD	Total Demand Distortion
THD	Total Harmonic Distortion
WTHD	Weighted Total Harmonic Distortion
VSC	Voltage source converter

Contents

1 Introduction **1**
- 1.1 Problem Statement . . . 1
- 1.2 Objectives . . . 1
- 1.3 Success criteria . . . 2
- 1.4 Methodology . . . 2
- 1.5 Limitations and Scope . . . 2
- 1.6 Thesis Outline . . . 3

2 State of the Art **5**
- 2.1 Harmonic Power Quality Analysis . . . 5
- 2.2 Standards . . . 6
- 2.3 E□ects of Harmonics . . . 8
- 2.4 Resonances . . . 9
- 2.5 Filters . . . 10
  - 2.5.1 Passive Filters . . . 10
- 2.6 Summary . . . 13

3 Harmonic Analysis of Converters **15**
- 3.1 Three-phase Graetz-bridge Converter . . . 15
- 3.2 Two-level PWM Converter . . . 17
- 3.3 Harmonic Impedance and Load flow . . . 20
- 3.4 Modeling of Converters . . . 20
- 3.5 Harmonic Injections . . . 21
  - 3.5.1 Balanced, Phase Correct . . . 21
  - 3.5.2 IEC 61000 . . . 21
- 3.6 Summary . . . 22

4 Study Cases **23**
- 4.1 External Grid Parameters . . . 24
- 4.2 Transformer . . . 24
- 4.3 Cables . . . 24
- 4.4 Loads . . . 25
- 4.5 Generators . . . 25
- 4.6 Converter Harmonic Assumptions . . . 25
  - 4.6.1 Photovoltaic System . . . 26
  - 4.6.2 Electric Vehicle Charger . . . 26
- 4.7 EV Charger Filter Design . . . 27
- 4.8 Cases . . . 30
  - 4.8.1 Base Case . . . 30
  - 4.8.2 Case 1 - PV System 2 (80[%] and 100[%] PV Capacity - Terminal 8) 34
  - 4.8.3 Cases 2 - 4 - EV Cases . . . 35

4.8.4 Case 4 - Maximum EV on Terminal 8 40
4.8.5 Case 5 - 270 [kW] PV System on Terminal 8 and Four 50 [kVA] EV Chargers 41
4.9 Modeling Converter as an Equivalent Source 43
4.10 Summary 47

5 Conclusions and Future Work **49**

6 Appendix **51**

Bibliography **53**

1 Introduction

Due to environmental goals adopted by the European Council in October 2014 [1] (at least 40[%] cuts in greenhouse gas emissions from 1990 levels, 32[%] share for renewable energy and decreasing market prices, and 32.5[%] improvement in energy efficiency), changes are expected in fossil fuel consumption and self-production of electricity. It may soon be common for households to have more high-power converters such as electric vehicle (EV) chargers, photovoltaic (PV) inverters, and battery inverters. As the trend of power-electronic-interfaced distribution energy resources (DER) is increasing, power quality in low-voltage grids becomes a more critical issue.

Power quality is a broad topic that contains many aspects such as continuity of service, variations in voltage magnitude, voltage, and current transients, harmonic content, and phase imbalances [2]. Harmonics created by power-electronics based equipment is the main focus of this study. The highly nonlinear loads modify the sinusoidal nature of the voltage and current in the grid. Power-electronics based converters inject harmonics into the network, which can affect sensitive loads and meters [3]. Moreover, they can alter the operation of other devices, which is further explained in Chapter 2.

There are different metrics to assess harmonic distortions, e.g., total harmonic distortion (THD) and total demand distortion (TDD), as described in electrical standards such as IEEE 519 [3]. Power converters used in homes have to limit their harmonic output according to standards such as IEEE (Institute of Electrical and Electronics Engineers) 519 [3] and IEC (International Electrotechnical Commission) 61000 [4]. However, there might be a significant effect on power quality when many are active in the same feeder. Some of the main issues caused by harmonics include losses and interference with the regular operation of devices. Studies have shown that a high penetration of power electronic devices such as PV and EV can increase the harmonic content in distribution grids [5, 6]. Therefore, it is essential to determine if the current power quality standards and converter harmonic outputs are sufficient for the distribution grids in the future.

1.1 Problem Statement

How do solar PVs, electric vehicle charging stations, and battery storage affect the power quality of a distribution grid?

1.2 Objectives

The following objectives are established to answer the problem statement:

- Assessment and control of harmonic power quality in the grid with varying conditions:
  - Penetration levels of PV, EV, and battery storage
  - Converter topologies
- Suggest a solution for mitigation or regulation of power quality problems in a distribution grid to meet the standards

1.3 Success criteria

- THD_v and TDD meet the standard requirements
- Individual harmonics do not violate the respective standards
- Voltage deviation stays within the chosen limits (+/- 0.1 [pu]) [7]

1.4 Methodology

The grid contains household PVs, battery storage, EV charging stations, and general loads. The analysis is performed using the harmonic load-flow and frequency sweep. First, the simulation model is developed based on the low-voltage (LV) European benchmark grid [8]. Different variations of the model are created for varying penetration levels and combinations of the power-electronics-based converters.

Harmonic analysis is performed to determine the impact on individual voltage and current harmonics, THD and TDD. It consists of power quality measurements at a few points in the low-voltage grid and at both sides of the step-up transformer. The harmonic analysis is compared to the limits set by standards to determine if there are power quality violations. If the limits are breached, a passive filter at the nonlinear load is designed to mitigate the issues. The recommendation of how to mitigate and/or regulate power quality is proposed in terms of which harmonics are generated and absorbed by the different devices with a focus on the converters.

1.5 Limitations and Scope

The study focuses on the harmonic power quality in a distribution grid with varying penetrations of PV, EV, and battery storage. Limitations are taken into account:

- Only steady-state conditions are considered, and the energization scheme is omitted.
- Only 3-phase Graetz-bridge converters and two-level voltage source converters (VSC) are considered.
- Interharmonics are not considered.
- Frequency deviation is not considered.
- Generic converter models available in the Powerfactory library are used.
- The cables are modeled with distributed-line parameters.
- Transformer saturation and motor loads are not considered.

The scope of the study is observing the harmonic power quality in a distribution grid with varying penetration levels of power-electronics-based converters. The study analyzes balanced steady-state simulation and harmonic load flow. The PV and EV converters are considered as unidirectional. Battery storage and PV use similar inverters, so they are

considered together. Moreover, different output levels are taken into consideration for the PV inverters.

1.6 Thesis Outline

A summary of each chapter is given below:

The first chapter introduces the motivation for this study. It also includes the objectives and methodology of the study.

Chapter 2 provides further analysis of previous studies. Power quality metrics are defined for the study. Standards that are used for validating simulation results are introduced and defined. The main issues resulting from harmonics in distribution grids are explored. The resonance phenomenon is detailed along with circuit examples. Harmonic filtering which is used throughout the study is explained.

Chapter 3 describes the converter topologies used in this study and their characteristic harmonic components. These include the Graetz-bridge converter and two-level PWM inverter. Modeling of the converters and harmonic injections are described. The method of harmonic analysis used in Chapter 4 is also described.

Chapter 4 presents the grid model used in the study cases along with the simulation results. The study cases explore the effect of adding nonlinear loads with harmonic distortions, and how to minimize them. The grid model and components are thoroughly detailed. The filter design for the modeled EV chargers is explained and analyzed. Results from the study cases are shown and described.

Chapter 5 summarizes the conclusions from the study, discusses the impact of the study. In addition, it lists some of the future studies that could continue this work.

State of the Art 2

A few decades ago, electric power mainly flowed from big thermal plants through transmission systems to loads in distribution grids. Since that time, more and more distributed renewable energy sources (RES) have been installed along with the shutdown of thermal plants. PVs, EVs, and battery storage are becoming more popular at the distribution level, which moves some generation and storage to distribution grids. EVs can be sizeable nonlinear loads with usual in-home rated charging powers around 3.6-24 [kW]. Higher power chargers are available, but require large current capacities. Existing EVs have the option to be charged by different chargers. There are single-phase and three-phase chargers, with the unidirectional or bidirectional converters dependent on the car model. PV solar panels with a battery can connect to the grid through a hybrid inverter, which includes a DC-DC converter between the battery and solar panels. Distribution grids face power quality problems from the increase in nonlinear devices. Whenever energy flows through them, harmonics are generated because of changes to the sinusoidal nature of grid voltage and current.

2.1 Harmonic Power Quality Analysis

There are various existing metrics to evaluate the power quality of a distribution grid. The commonly used metrics are related to the distortion of the voltage and current waveforms from their ideal sinusoidal shape. Individual voltage and current harmonic components can be evaluated. The combination of all harmonics gives an overall picture of the harmonic power quality. Total harmonic distortion provides a metric for the distortion of the sinusoidal grid voltage or current by all integer-multiple harmonic components with respect to the fundamental component. THD is defined as

$$THD = \frac{1}{f_1} \sum_{h=2}^{\infty} \sqrt{f_h^2} \tag{2.1}$$

where f_h is the root-mean-square (RMS) amplitude of the h-th order voltage or current harmonic, f_1 is the RMS of the fundamental component.

The weighted total harmonic distortion is weighted inversely with frequency and is defined as

$$WTHD = \frac{1}{f_1} \sum_{h=2}^{\infty} \sqrt{\left(\frac{f_h}{h}\right)^2} \tag{2.2}$$

Since the THD for current can be misleading when the loading is light, total demand distortion can also be evaluated. TDD provides a metric for the distortion of sinusoidal

current by harmonics with respect to rated/maximum current. TDD is defined as

$$TDD = \frac{1}{I_{max}} \sum_{h=2}^{\infty} \sqrt{I_h^2} \tag{2.3}$$

where I_h is the RMS amplitude of the h-th order current harmonic, and I_{max} is the rated current. The relevant standards usually consider harmonics up to around the 40th or 50th order.
To explain power quality issues, it is worth mentioning the relation between voltage harmonics and current harmonics. Current harmonics appear by the nonlinear loads, when the drawn current is not sinusoidal i.e. rectifier. When the waveform is not sinusoidal, it can be represented by the Fourier series. Voltage harmonics are mostly generated by current harmonics. Voltage sources are distorted by the current harmonics due to system impedance causing voltage drops across impedances, which distort voltage waveform.

2.2 Standards

There are standards such as IEEE 519, IEEE 1547, IEC 61000, and EN 50160 to maintain the power quality in the grid. IEEE 519 includes recommended limits for voltage harmonics measured in electric grids at multiple voltage levels and current distortion limits for loads and generators. The IEEE 519 limits for voltage harmonic distortion in a distribution grid are given in Table 2.1. Table 2.2 presents the individual voltage harmonic limits in public low-voltage networks according to IEC 61000-2-2. EN 50160 describes voltage quality limits in Europe, including voltage variations, dips, phase imbalance, and harmonic levels [7]. The 10[%] supply voltage variation limit in normal operation from this standard is implemented in this study. A summary of the relevant harmonic power quality limits in a distribution grid is presented in Tables 2.1-2.5.

Table 2.1: IEEE Standard 519-2014: voltage distortion limits [3]

Voltage Level	Individual Voltage Distortion	Total Voltage Distortion
V $\leq$ 1 kV	5%	8%
1 kV < V <69 kV	3%	5%

Table 2.2: IEC 61000-2-2: voltage distortion limits in public low-voltage networks [9]

Odd harmonics		Even harmonics		Triplen harmonics	
Order (h)	V_h(%)	Order (h)	V_h(%)	Order (h)	V_h(%)
5	6	2	2	3	5
7	5	4	1	9	1.5
11	3.5	6	0.5	15	0.3
13	3	8	0.5	$\geq$ 21	0.2
17	2	10	0.5		
19	1.5	$\geq$ 12	0.2		
23	1				
25	1.5				
$\geq$ 29	0.2+12.5/h				

IEEE 519:2014 also gives limits for current harmonics in distribution systems, as shown in Table 2.3. PV inverters are required to meet harmonics standards such as IEEE 1547 [10] in order to receive certification, shown in Table 2.4. The limits are similar to the ones presented in Table 2.3 with small differences in the even harmonic components. IEC 61000-3-2 sets maximum current limits of individual harmonics (up to the 40th harmonic) for converters operating with input current up to 16 [A] per phase in low-voltage distribution grids, as shown in Table 2.5.

Table 2.3: Current distortion limits for systems rated 120 [V] through 69 [kV] according to IEEE 519:2014 [3]

Maximum harmonic current distortion in percent of I_L						
	Individual harmonic order (odd harmonics)[a,b]					
I_{sc}/I_L	3 $\leq$ h <11	11 $\leq$ h <17	17 $\leq$ h <23	23 $\leq$ h < 35	35 $\leq$ h < 50	TDD
<20[c]	4.0	2.0	1.5	0.6	0.3	5.0
20<50	7.0	3.5	2.5	1.0	0.5	8.0
50<100	10.0	4.5	4.0	1.5	0.7	12.0
100<1000	12.0	5.5	5.0	2.0	1.0	15.0
>1000	15.0	7.0	6.0	2.5	1.4	20.0

[a] Even harmonics are limited to 25% of the odd harmonic limits above
[b] Current distortions that result in a dc offset, e.g., half-wave converters, are not allowed
[c] All power generation equipment is limited to these values of current distortion, regardless of actual Isc/IL.
where Isc = maximum short-circuit current at PCC
I_L = maximum demand load current (fundamental frequency component) at the PCC under normal load operating conditions

The odd-harmonic limits in Table 2.3 are increased for converters using higher pulses with a multiplier defined as

$$Multiplier = \sqrt{\frac{p}{6}}, \tag{2.4}$$

where p is the number of pulses.

Table 2.4: IEEE Standard 1547-2018 [10]: PV inverter current distortion limits

Maximum harmonic current distortion in percent of I_{rated} [a]						
Individual odd harmonic order h	h <11	11 $\leq$ h <17	17 $\leq$ h <23	23 $\leq$ h <35	35 $\leq$ h <50	TRD
Percent (%)	4.0	2.0	1.5	0.6	0.3	5.0
Individual even harmonic order h	h = 2	h = 4	h = 6	8 $\leq$ h <50		
Percent (%)	1.0	2.0	3.0	Associated range specified for odd harmonics		

[a] I_{rated} = the DER unit rated current capacity (transformed to the RPA when a transformer exists between the DER unit and the RPA).
TRD = The total root-sum-square of the current distortion components (including harmonics and inter-harmonics) created by the DER unit expressed as a percentage of the DER rated current capacity (I_{rated}).

Table 2.5: IEC 61000-3-2: individual current harmonic limits for Class A equipment ($\leq$ 16 [A] per phase)

Odd harmonics		Even harmonics	
Order (h)	Current (A)	Order (h)	Current (A)
3	2.3	2	1.08
5	1.14	4	0.43
7	0.77	6	0.3
9	0.4	8 $\geq$ h $\leq$ 40	$0.23\frac{8}{h}$
11	0.33		
13	0.21		
15 $\geq$ h $\leq$ 39	$0.15\frac{15}{h}$		

2.3 E□ects of Harmonics

Harmonics have been found to cause issues in distribution grids, among others [2, 5]:

- Heating and losses in transformers
- Interference with communication devices
- A decrease in the lifetime of electrical devices
- Additional losses in electrical machines
- Overloading of the neutral conductor
- False tripping of protection equipment

The integration of PV in distribution grids has been found to increase harmonic levels above the accepted limits in IEEE 519 [5, 6]. The THD of PV inverters are also higher when the output is lowered, e.g., on cloudy days [6, 11, 12]. The increase of PV penetration in low-voltage grids increases the load capacitance and lowers the resonant frequency seen

by the transmission network. This leads to a decrease in the lower-order harmonic damping ability [13]. Adding passive filters at the outputs of PV inverters and EV charging stations is shown to decrease THD in a distribution grid [14].

In [15], a method to assess the impact of plug-in hybrid electric vehicles (PHEV) on the power system's power quality with the two-phase network (U.S. model) was established. The paper analyzed different slow charger types available in the market, which showed that the voltage third harmonic has the highest magnitude, with the notification that harmonic distortion caused by PHEV is not significant in the primary network. On the contrary, it was mentioned that a single-phase charger caused a rise of the neutral-to-earth voltage at the fundamental frequency in the secondary network. In [16], it was depicted that for fast-charging stations, the fifth harmonic component has the highest magnitude. What is more, the fifth-harmonic current did not change proportionally to the fundamental current during the charging state, which means when the fundamental current decreased in the later stage, the harmonic current became significant.

Moreover, the number of EVs connected to the grid matters [17]. This study concluded that an increased number of EVs resulted in higher values of THD_v and THD_i. Electric vehicles harmonic currents have a lower impact on the harmonic distortion level while being connected in proximity to a service transformer. In other words, the higher the short-circuit level, the less noticeable is the impact of the harmonic currents [18].

2.4 Resonances

The issue with resonance in a power system is that at specific frequencies, the combined impedance of inductive and capacitive components can lead to unintended harmonic distortion. In power systems, there are two types of resonances: series and parallel. Two example resonance circuits are shown in Figure 2.1.

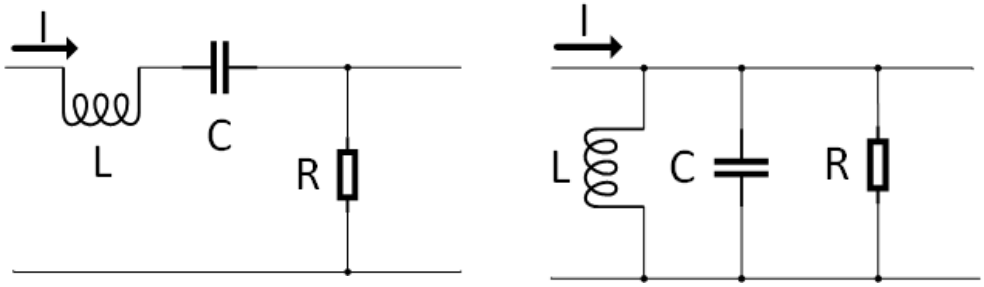

(a) Series resonance circuit

(b) Parallel resonance circuit

Figure 2.1: Resonance example circuits

The resonance between an inductor and capacitor occurs at resonance frequency, ω_n, defined by

$$\omega_n = \frac{1}{\sqrt{LC}} \tag{2.5}$$

In the parallel resonance circuit operating near the resonance frequency, the combined impedance of the inductor and capacitor branch becomes

$$Z = \frac{j\omega L(1/j\omega C)}{(j\omega L + 1/j\omega C)} = \frac{L/C}{j(\omega L - 1/\omega C)} \tag{2.6}$$

The combined impedance of the parallel circuit has a maximum of the resistor value, R, at the resonance frequency. This also leads to amplification of currents near the resonance frequency and potential nuisance fuse operation. The effect can be very damaging when the resonance frequency occurs around load-generated harmonic frequencies, e.g. fifth and seventh. Parallel resonances can appear between system impedance and capacitive elements such as power capacitors.

In the series resonance circuit, the resonance frequency is also defined as in (2.5), but the effect is slightly different. The series impedance of the RLC circuit has a minimum of R at the resonance frequency, shown by

$$Z = R + j(\omega L - \frac{1}{\omega C}) \tag{2.7}$$

This provides a low impedance path for harmonic currents, which in turn can potentially generate large voltage distortions. Series resonance can arise in situations such as [19]:

- a capacitor bank and line or transformer reactance
- capacitive impedances of cables and long lines (usually around 5-15 [kHz])
- series compensation of power lines

The utilization of series resonance is to reduce harmonics by providing a low-impedance path to ground. On the other hand, parallel resonance is an unintended phenomenon, which can result in a situation when a small current produces excessive voltage at the resonant frequency.

2.5 Filters

To meet power quality criteria such as the ones mentioned in Section 2.2, multiple harmonics mitigation techniques have been proposed since the problem appeared. Converters must comply with standards such as the ones in Section 2.2, usually with the help of filters. Depending on the scale of the power quality issues, passive and active filters are available. Active filters use power-electronic components to cancel harmonics, but can also emit interharmonics. "Interharmonic (component): A frequency component of a periodic quantity that is not an integer multiple of the frequency at which the supply system is operating (e.g., 50 [Hz] or 60 [Hz])." [3].

2.5.1 Passive Filters

Passive filters consist of only passive components: capacitors, inductors, and resistors. The goal of passive filters is to absorb the unwanted harmonic currents, thus reducing the harmonic current that are injected into the grid and improving the power quality. Passive

shunt filters provide a low impedance path to ground for harmonic distortions by utilizing the series resonance phenomenon. This effect is explained with the use of Figure 2.2, which shows how harmonic currents I_h are split between the shunt filter Z_{sh} and the grid impedance Z_g.

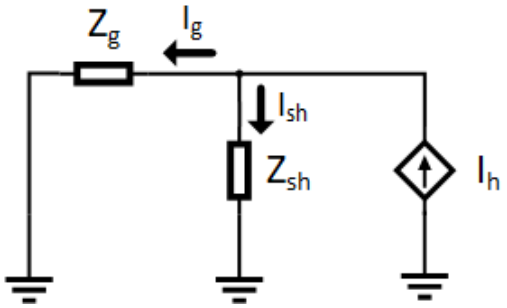

Figure 2.2: Division of harmonic current between filter and grid

The harmonic current flowing to the shunt filter is calculated as

$$I_{sh} = \frac{Z_g}{Z_g + Z_{sh}} I_h = \rho_f I_h \tag{2.8}$$

where ρ_f is the proportion of filter current to generated harmonic current for a specific harmonic frequency.

One method of categorizing passive filters is to split them in the following manner:

- Single-tuned (ST) filter
- Double-tuned (DT) filter
- High-pass (Damped) filter

Dependent on the filter type, it can be for a specific frequency (single-tuned) or for a range of frequencies (damped). Typically, damped filters are used to reduce higher-order harmonics starting near and above the tuned frequency. To keep the losses at low values, single- and double-tuned filters are utilized for low-order harmonics, because their resistance is lower than the damped filters. The layouts and impedance characteristics of a single-tuned and second-order damped filter are shown in Figures 2.3 and 2.4 respectively.

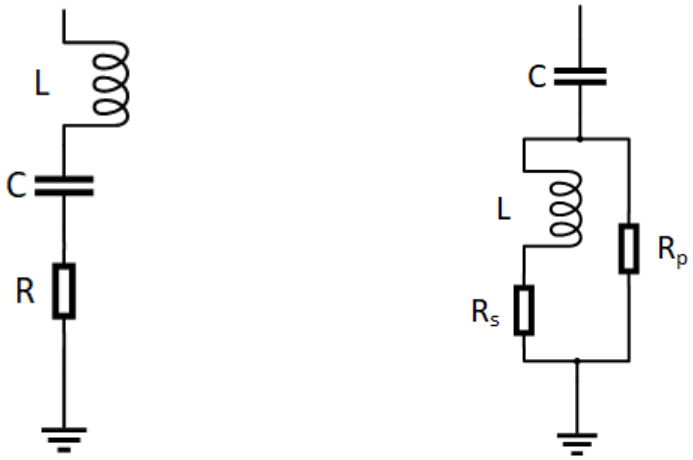

(a) Single-Tuned Filter Impedance Layout (b) Second-Order High-Pass Filter Layout

Figure 2.3

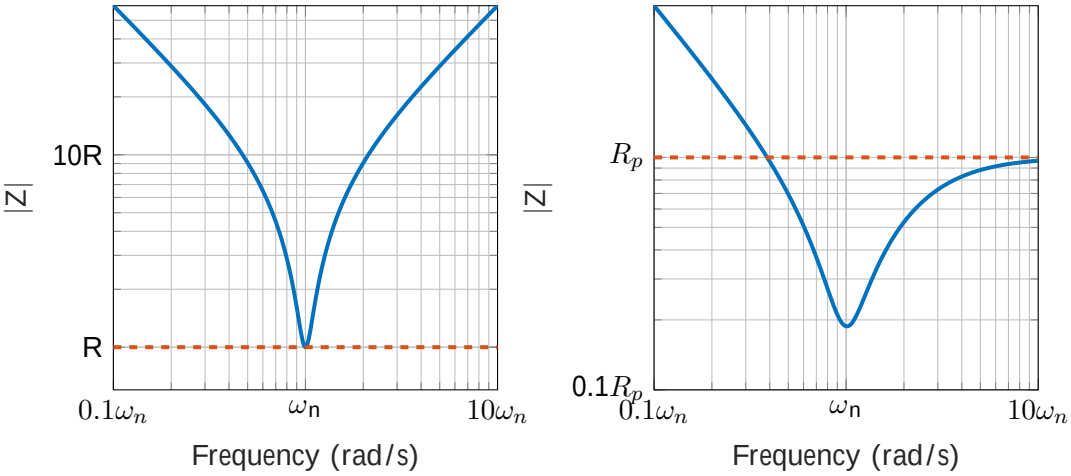

(a) Single-Tuned Filter Impedance vs. Frequency (b) Second-Order High-Pass Filter Impedance vs. Frequency

Figure 2.4

Six-pulse converters are typically filtered using a hybrid combination of tuned branches for low-order harmonics and a high-pass damped filter for the 17th and higher orders [20]. In [21], different passive filters are described with the design for three-phase PV grid-connected inverters.

Single-tuned Filter

Single-tuned filters are generally tuned to low-order characteristic harmonics. The filter impedance can be represented in (2.7) since the ST filter uses series resonance to absorb harmonic distortions. The second term becomes zero at the resonance frequency defined in (2.5), resulting in a path of low impedance equal to the resistance (R). By adding more parallel branches in the filter, resonances can be added at more harmonic frequencies.

The relative frequency deviation δ is given as

$$\delta = \frac{\omega - \omega_n}{\omega_n} \tag{2.9}$$

The quality factor (QF) of a filter is related to the sharpness of the tuning, or the slope of the impedance near the resonance frequency. The QF of a single-tuned filter is the ratio of reactance to resistance at the resonance frequency, given as

$$QF = \frac{\sqrt{L/C}}{R} = \frac{X_0}{R} \tag{2.10}$$

A high-quality ST filter refers to one that is sharply tuned to a harmonic frequency, usually with QF ranging between 30 and 60 [20]. The impedance of the filter near the resonance frequency can also be expressed in terms of QF, δ, and R as

$$Z \approx R(1 + j2\delta QF) \tag{2.11}$$

This can also be rewritten for admittance as

$$Y \approx \frac{1}{R(1 + j2\delta QF)} = \frac{QF}{X_0(1 + 4\delta^2 QF^2)} - j\frac{2\delta QF^2}{X_0(1 + 4\delta^2 QF^2)} \tag{2.12}$$

The reactive power output by a single-tuned filter at the fundamental frequency is

$$Q = \frac{V^2}{X_C - X_L} \tag{2.13}$$

where V is the terminal voltage, and X_L and X_C are the capacitive and inductive reactances, respectively.

High-pass (Damped) Filter

The impedance of the damped filter in Figure 2.3b is equivalent to

$$Z = \frac{1}{j\omega C} + (\frac{1}{j\omega L + R_s} + \frac{1}{R_p})^{-1} \tag{2.14}$$

This filter is designed to absorb high-frequency harmonic distortions. For high-pass filters, the quality factor is measured as the reciprocal of how it measured for single-tuned filters.

$$QF = \frac{R_p}{\sqrt{L/C}} = \frac{R_p}{X_0} \tag{2.15}$$

2.6 Summary

This chapter highlights few important aspects in regards of assessment of harmonics in the grid. Firstly, the common metrics and di□erent standards in power quality studies are

presented. Later, the negative effects of harmonics and potential risks are enumerated. Furthermore, the resonance phenomenon and filtering is presented. The filters section defines the filter types utilized in the study.

Harmonic Analysis of Converters 3

In order to understand and discuss harmonics, Fourier series analysis is used. A Fourier series representation is sufficient to represent any periodic function, which can be decomposed into a summation of harmonic components [22].

Fourier series of a periodic function $f(x)$ of period T is:

$$f(x) = a_0/2 + \sum_{h=1}^{\infty} a_h \cos(2\pi hx/T) + \sum_{h=1}^{\infty} b_h \sin(2\pi hx/T) \tag{3.1}$$

The term $2\pi/T$ represents the fundamental frequency of the periodic function $f(t)$. The term $h2\pi/T$ is the h-th harmonic term of $f(t)$. The a_0, a_h, b_h are called coefficients of $f(x)$.

$$a_0 = 2/T \int_0^T f(x)dx \tag{3.2}$$

$$a_h = 2/T \int_0^T f(x)\cos 2\pi hx/T dx \tag{3.3}$$

$$b_h = 2/T \int_0^T f(x)\sin 2\pi hx/T dx \tag{3.4}$$

3.1 Three-phase Graetz-bridge Converter

One typical three-phase converter uses thyristors in the full-bridge configuration. The circuit layout is shown in Figure 3.1.

The characteristic current harmonics are obtained by analyzing the ideal dc circuit, where $i_d = I_d$, $L_s = 0$, and $L_d = 0$. The quasi-square wave current through one phase is represented in Figure 3.2.

The two other phase currents are similar but offset by $\pm$ 120 degrees. Using (3.2 - 3.4), the Fourier coefficients of the current waveform are

$$a_0 = 0, \quad a_h = 0, \quad b_h = \frac{4I_d}{h\pi} cos(h\frac{\pi}{6}) \qquad \text{where } h \text{ is all odd integers} \tag{3.5}$$

The results of this lead to the following relationship between the RMS value of the fundamental-frequency and h-th order component:

$$I_{s1} = \frac{2I_d}{\pi}\sqrt{\frac{3}{2}} \approx 0.78 I_d \tag{3.6}$$

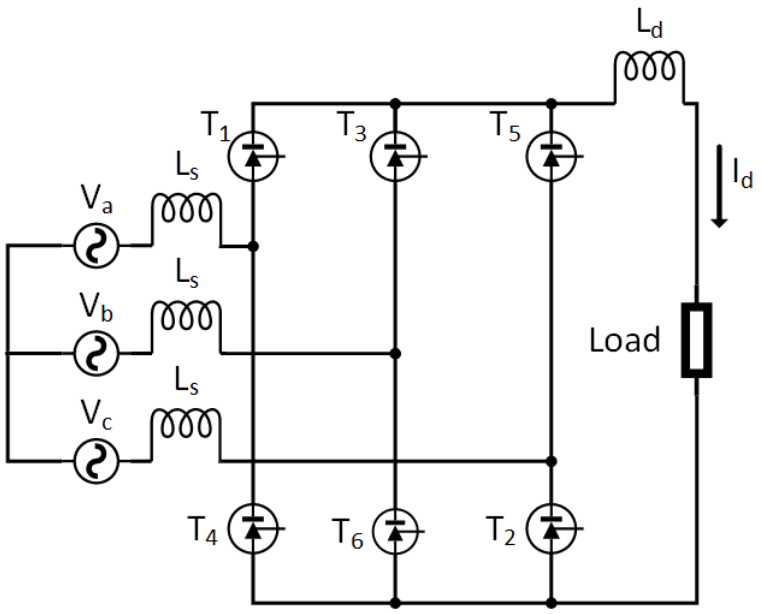

Figure 3.1: Three-phase thyristor converter layout

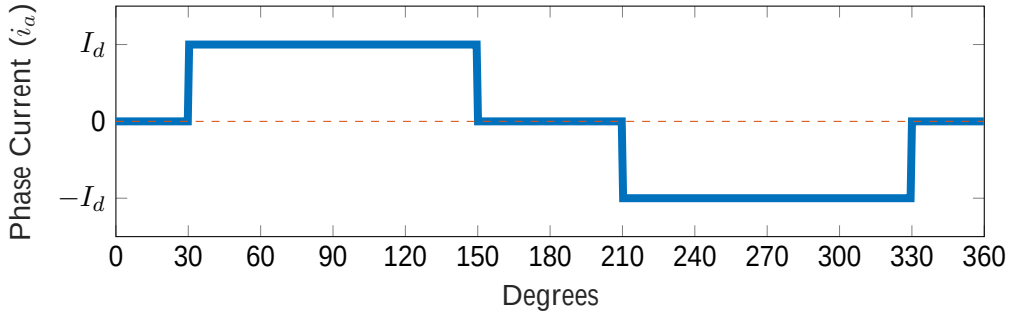

Figure 3.2: Ideal phase current

$$I_{sh} = \frac{I_{s1}}{h} \qquad for\ h = 6n \pm 1 \tag{3.7}$$

The phase current i_s contains only odd nontriplen harmonic components and can be expressed in the Fourier representation as

$$\begin{aligned} i_s = &\sqrt{2}I_{s1}sin(\omega_1 t) - \sqrt{2}I_{s5}sin(5\omega_1 t) - \sqrt{2}I_{s7}sin(7\omega_1 t) \\ &+ \sqrt{2}I_{s11}sin(11\omega_1 t) + \sqrt{2}I_{s13}sin(13\omega_1 t) - ..., \end{aligned} \tag{3.8}$$

where I_{sh} is the RMS amplitude of the current for the h-th order harmonic, and ω_1 is the fundamental frequency in [rad/s]. More harmonics are added to the characteristics when considering nonideal circuits with inductance.

A twelve-pulse converter contains two six-pulse converters, with one phased shifted 30°, which cancels the harmonics in (3.7) where n is odd. The characteristic current equation for a twelve-pulse converter is

$$i_s = \sqrt{2}I_{s1}sin(\omega_1 t) - \sqrt{2}I_{s11}sin(11\omega_1 t) + \sqrt{2}I_{s13}sin(13\omega_1 t) - \sqrt{2}I_{s23}sin(23\omega_1 t) + \sqrt{2}I_{s25}sin(25\omega_1 t) - ..., \tag{3.9}$$

The harmonic spectrums of ideal six- and twelve-pulse converter circuits are shown in Figure 3.3.

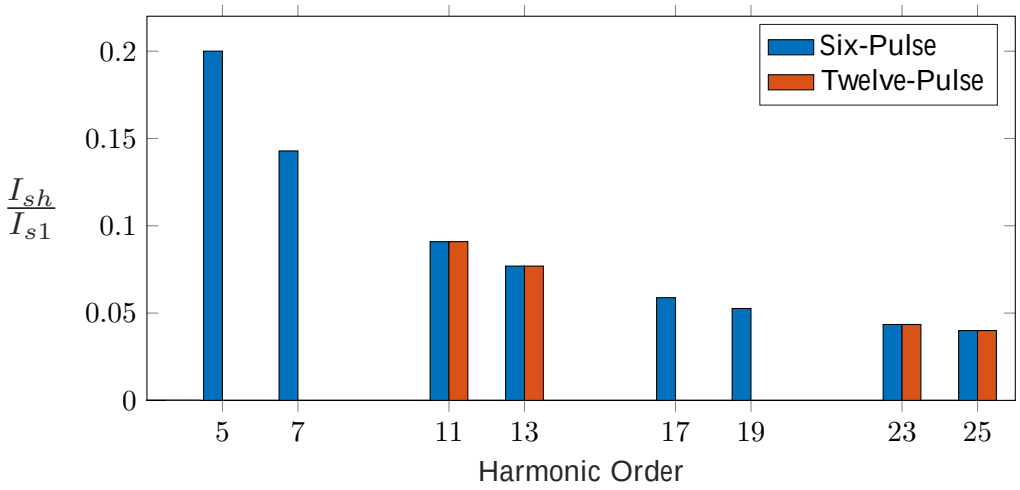

Figure 3.3: Current harmonic spectrum of ideal six- and twelve-pulse full-bridge thyristor converters

The THD_i of the ideal six-pulse converter is calculated using (2.1) as

$$THD_i = \sqrt{\frac{\pi^2}{9} - 1} = 31.08[\%] \tag{3.10}$$

The THD_i of the ideal twelve-pulse converter is calculated using (2.1) as

$$THD_i = 15.22[\%] \tag{3.11}$$

3.2 Two-level PWM Converter

In the three-phase pulse-width-modulated (PWM) inverter operation, the objective is to shape and control the output voltages in magnitude and frequency with constant input voltage V_d. In order to get balanced three-phase output voltages, the triangular carrier voltage waveform is compared with three sinusoidal control voltages, which are shifted by $\pm$ 120 degrees. The two-level converter circuit layout is shown in Figure 3.4.

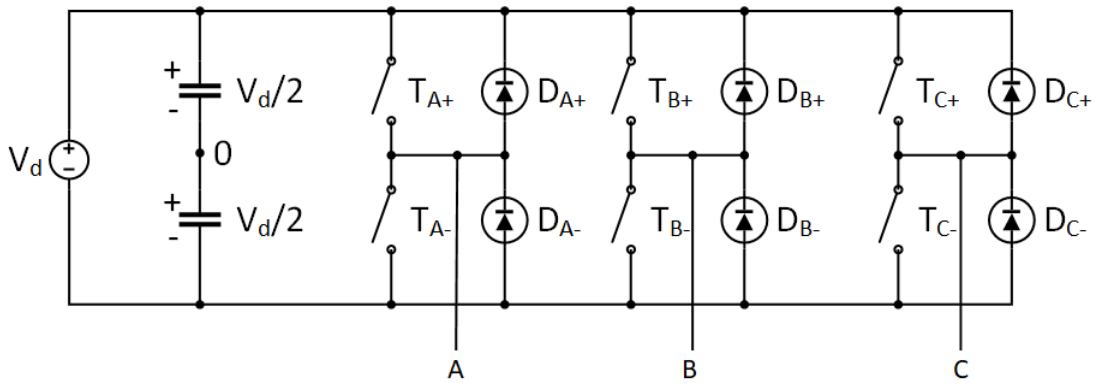

Figure 3.4: Two-level PWM converter layout

In order to eliminate the even harmonics, the triangular waveform signal and the control signal should be synchronized to each other. It requires the modulation ratio m_f to be an integer, otherwise subharmonics would be generated. Subharmonics are distortions at frequencies below the fundamental. The ideal phase-to-zero voltage of a naturally sampled two-level PWM (triangular carrier) converter is presented as

$$\begin{aligned} V_{a0}(t) &= \frac{V_d}{2} + \frac{V_d}{2} M \cos \omega_0 t \\ &+ \frac{4V_d}{\pi} \sum_{m=1}^{\infty} \sum_{n=-\infty}^{\infty} \frac{1}{m} J_n(\frac{mM\pi}{2}) \sin\left([m+n]\frac{\pi}{2}\right) \cos\left(m\omega_c t + n\omega_0 t\right) \end{aligned} \tag{3.12}$$

where M is the modulation index, m is the carrier index, n is the baseband index, ω_0 is the fundamental angular frequency, ω_c is the carrier angular frequency, and J refers to the Bessel function of the first kind. The characteristic harmonics are composed of three main components:

- the fundamental component $V_d M$ (m = 0, n = 1)
- the carrier harmonics ($m = 1$ to ∞, n = 0)
- the sideband harmonics ($m = 1$ to ∞, n= -∞ to ∞ excluding n = 0)

The characteristic voltage harmonics of two-level PWM converters are the largest at orders around the carrier harmonics (integer-multiple harmonics of the modulation ratio).

In the three-phase two-level converter, the line-to-line voltage harmonics are typically analyzed. Triplen harmonics can be eliminated by selecting an odd modulation ratio that is a multiple of three. The line-to-line voltage is

$$\begin{aligned} V_{ab}(t) &= \sqrt{3}\frac{V_d}{2} M \cos(\omega_0 t + \frac{\pi}{6}) \\ &+ \frac{4V_d}{\pi} \sum_{m=1}^{\infty} \sum_{n=-\infty}^{\infty} \frac{1}{m} J_n(\frac{mM\pi}{2}) \sin\left([m+n]\frac{\pi}{2}\right) \sin(n\frac{\pi}{3}) \cos\left(m\omega_c t + n[\omega_0 t - \frac{\pi}{3}] + \frac{\pi}{2}\right) \end{aligned} \tag{3.13}$$

The ideal harmonic spectrum of the phase-to-zero voltage is shown in Figure 3.5.

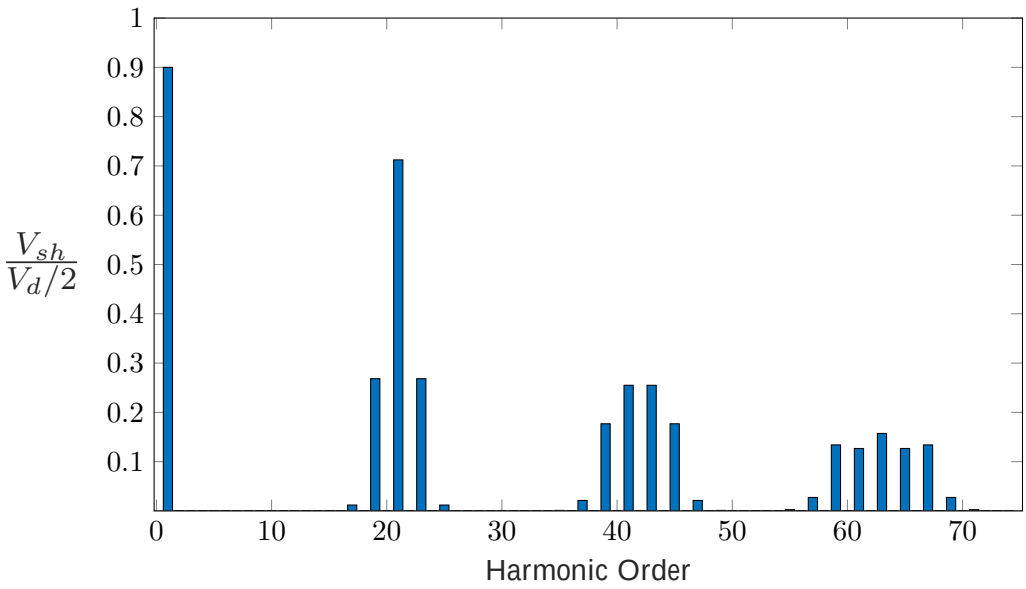

Figure 3.5: Phase-to-zero Voltage harmonic spectrum of an ideal naturally sampled two-level PWM converter with triangular modulation (modulation index M = 0.9, modulation ratio ω_c/ω_0 = 21)

The THD_v of the phase-to-zero voltage waveform up to the 50th harmonic is about 242[%]. The ideal line-to-line voltage harmonic spectrum of the two-level PWM is shown in Figure 3.6. The THD_v of the line-to-line voltage waveform up to the 50th harmonic is about 124[%].

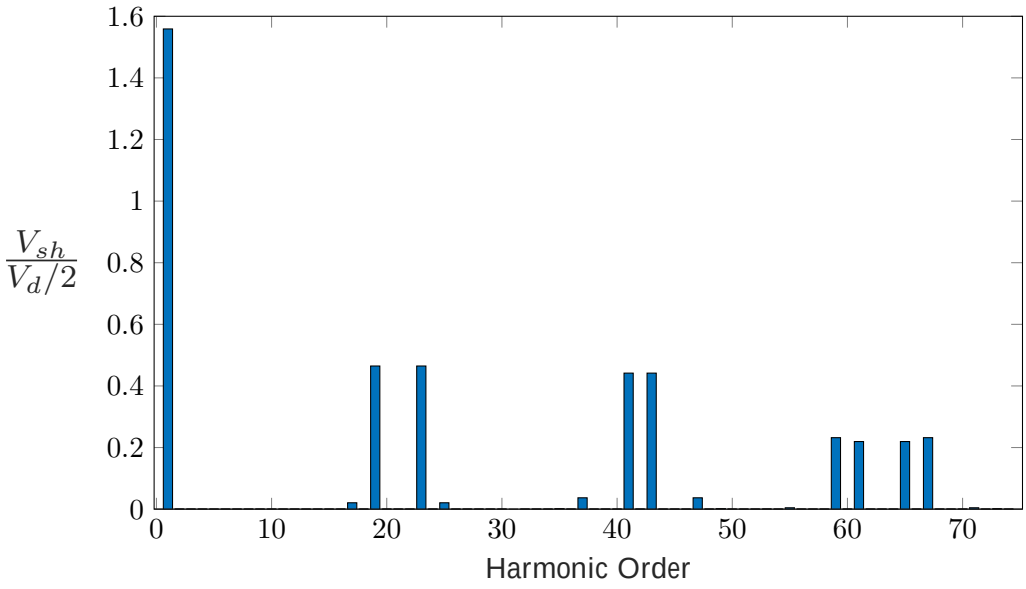

Figure 3.6: Line-to-line voltage harmonic spectrum of an ideal naturally sampled two-level PWM converter with triangular modulation (modulation index M = 0.9, modulation ratio ω_c/ω_0 = 21)

3.3 Harmonic Impedance and Load flow

Harmonic impedance is an important parameter in the context of power quality. It defines the voltage response of the system when it is a□ected by high-frequency currents. Any harmonic current generated by the load will cause voltage drop in the power supply impedance at the same harmonic frequency. The impedance can be split up to load impedance and supply system network impedance. The point where the public electricity supply grid connects to consumers is called the point of common coupling (PCC) [23]. The importance of the harmonic impedance is reflected upon the power system response and appropriate design of mitigation techniques, e.g., filters, since the system impedance increases as the frequency goes up. Powerfactory provides two functions to analyze the harmonics in the frequency domain:

- Harmonic Load Flow
- Frequency Sweep

"PowerFactory's harmonic load flow calculates harmonic indices related to voltage or current distortion, and harmonic losses caused by harmonic sources (usually non-linear loads such as current converters)" [24]. The harmonic load flow computes a network analysis at every frequency at which harmonic sources are defined.
Powerfactory's frequency sweep function carries out an analysis for continuous frequency domain. This is applicable to calculate the self- and mutual-network impedances, which are useful to identify the series and parallel resonances. The points of resonance are able to identify the frequencies at which harmonic currents generate significant harmonic voltages.

3.4 Modeling of Converters

Due to di□erent electrical design approaches of manufacturers, the convenient model to represent harmonic sources is established by means of Thevenin or Norton equivalent. Figure 3.7 shows the Thevenin and Norton equivalent circuits respectively.

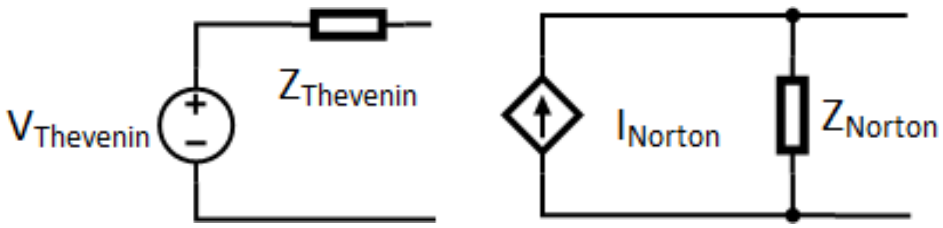

(a) Thevenin equivalent (b) Norton equivalent

Figure 3.7: Norton and Thevenin equivalent circuits

The harmonic components can also be modeled this way, with a sinusoidal voltage or current source for each harmonic order with corresponding amplitude, also known as harmonic indices. The Norton and Thevenin equivalent circuits are the dual of each other and one can be obtained from the other according to

$$\frac{V_{Thevenin}}{Z_{Thevenin}} = I_{Norton}, \quad Z_{Thevenin} = Z_{Norton} \tag{3.14}$$

The admittance of the Norton equivalent (G and B in parallel) could be replaced by the Thevenin equivalent impedance (R and X in series) as

$$Y = G + jB = Z^{-1}, \quad Z = R + jX \tag{3.15}$$

where Y is the admittance, G is the conductance, and B is the susceptance.

The Thevenin voltage represents the open-circuit voltage, while the Norton current equals the short-circuit current. These equivalents have more relevance in asymmetrical studies. An asymmetry happens when the magnitudes of phase voltages/currents are not equal and/or they are not in 120 degrees phase di□erence. It is convenient to represent an unbalanced system by three sets of components called positive, negative and zero sequence. That is why it is convenient to enter frequency-dependent impedances or admittances for each sequence.

Converters can be modeled by Norton or Thevenin equivalent circuits, usually depending on what characteristic harmonics are generated. For example, the six-pulse full-bridge converter's characteristic current harmonics given in Section 3.1 are easier to represent in the Norton configuration. On the other hand, the two-level PWM converter's characteristic harmonics described in Section 3.2 are easier to represent in the Thevenin configuration since the voltage components are given.

3.5 Harmonic Injections

The harmonic injections produced by nonlinear devices can be represented in multiple ways. In this study, "Balanced, Phase Correct", and "IEC 61000". Harmonic injection magnitudes are defined as a percentage of a reference value, either the fundamental component or the rated value. Devices defined by IEC 61000 can only have harmonic magnitudes referred to the rated value.

3.5.1 Balanced, Phase Correct

Harmonic sources can also be represented as "Balanced, Phase Correct". In this type, harmonic injections can be defined for positive and negative sequence integer harmonics. Triplen harmonics are not considered in this representation. Harmonic currents can be defined according to

$$I_h = k_h \cdot e^{\Delta\varphi_h} \cdot I_1 \cdot e^{h \cdot \varphi_1} \tag{3.16}$$

where k_h is I_h/I_{ref}, and φ_1 is the phase shift of the fundamental current component.

3.5.2 IEC 61000

The IEC 61000 type of harmonic injection can be used when the phase shifts of harmonic components are unknown. Therefore, the harmonic current injections are simply calculated as

$$I_h = k_h \cdot I_r \tag{3.17}$$

where I_r is the rated current of the device. IEC 61000-3-6 describes a "second summation law" that can be used for voltage or current as

$$U_h = \sqrt[\alpha]{\sum_{m=0}^{N} U_{h,m}^{\alpha}} \tag{3.18}$$

where U_h is the resultant harmonic voltage magnitude for the considered aggregation of N sources, m is the source index, and α is calculated in Table 3.1. In the harmonic load flow performed according to IEC 61000, triplen and non-integer harmonics are considered in the positive sequence.

Table 3.1: IEC 61000-3-6 summation exponent according to harmonic order

Alpha Exponent Value	Harmonic Order
1	h < 5
1.4	$5 \leq$ h ≤ 10
2	h > 10

3.6 Summary

The topologies of the six-pulse thyristor and two-level PWM converters are presented along with their characteristic harmonic components. An introduction to analyzing distribution grids is given through harmonic impedance and load flow, frequency sweep and harmonic injections implemented in Powerfactory.

Study Cases 4

The grid is based on the CIGRE European LV benchmark grid for renewable and DER [25], shown in Figure 4.1.

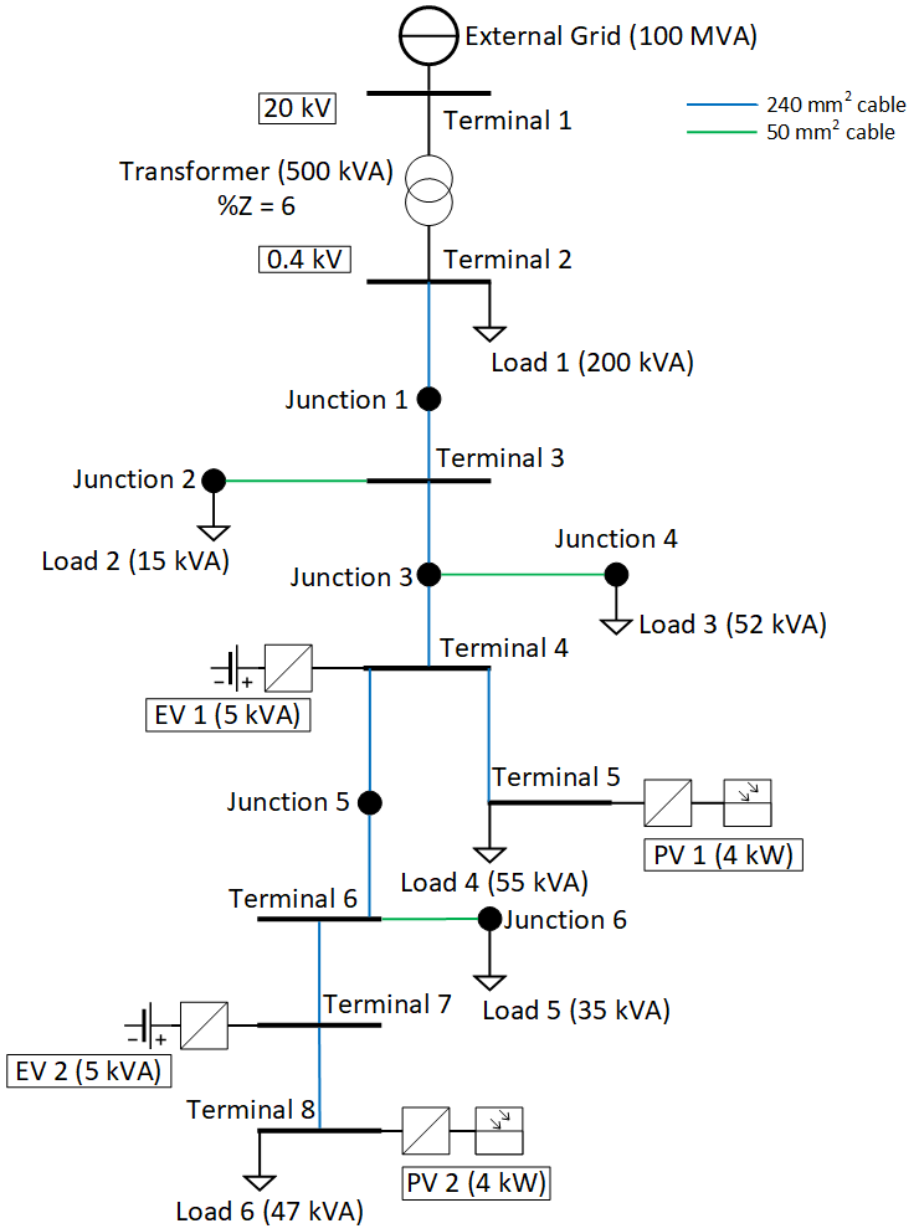

Figure 4.1: System drawing

The main parameters of the modeled grid components are given in the following sections.

4.1 External Grid Parameters

The external grid representing the rest of the grid is modeled with $100\ [MVA]$ short-circuit level and X/R ratio equal to 1 [25]. The background harmonics are modeled as a voltage source, shown in Table 4.2, based on [26].

Table 4.1: External Grid Parameters [25]

Name	Short-Circuit Power (MVA)	X/R Ratio
External Grid	100	1

Table 4.2: External Grid Harmonic Voltage Spectrum [26]

Harmonic Order	U_h (%)	Harmonic Order	U_h (%)
2	0.1	10	0.1
3	0.33	11	0.44
4	0.1	12	0.1
5	0.5	13	0.49
6	0.1	14 - 18	0.1
7	0.34	19	0.42
8	0.1	20 - 50	0.1
9	0.13		

4.2 Transformer

The transformer is based on a $0.5\ [MVA]$ generic model, the most similar to the CIGRE model. The parameters are shown in Table 4.3.

Table 4.3: Transformer Parameters

Parameter	Value
Rated Power	500 kVA
Primary-Side Voltage	20 kV
Secondary-Side Voltage	0.4 kV
Impedance (Secondary)	0.06 pu

4.3 Cables

The cables are modeled as distributed-parameter line models. They are modeled based on geometric data which in PF automatically includes frequency dependencies, because it calculates impedance and admittance matrices for the cable system for each harmonic load flow and frequency sweep. They are modeled based on the catalog [27] and [28] to be

as similar as possible to the CIGRE model [25]. The cables cross-sections are $240\ [mm^2]$ and $50\ [mm^2]$ and placed $0.9\ [m]$ underground. More details are given in the Appendix.

4.4 Loads

Loads in the feeder are defined in Table 4.4

Table 4.4: Loads

Name	**Load (kVA)**	**Power Factor (inductive)**
Load 1	200	0.95
Load 2	15	0.95
Load 3	52	0.95
Load 4	55	0.95
Load 5	35	0.95
Load 6	47	0.95
EV Charging Station 1 (Terminal 4)	5	0.95
EV Charging Station 2 (Terminal 7)	5	0.95

4.5 Generators

The EV charger load is represented as a static generator. In this project, EV charger loads consist of a unidirectional converter (6-pulse bridge), in other words, a rectifier. The PV inverter parameters are given in Table 4.5

Table 4.5: Sources Parameters

Converter	Rated Power (kVA)	Output Real Power (kW)	Output Reactive Power(kVAR)
PV Inverter 1 (Terminal 5)	4	4	0
PV Inverter 2 (Terminal 8)	4	4	0

4.6 Converter Harmonic Assumptions

Current harmonic distortions are shown as a ratio of harmonic current to fundamental current obtained from the load flow. Both the PV systems and EV chargers are modeled using the Norton equivalent. Initially, each Norton equivalent uses a large impedance to study the outgoing harmonics. Later, the PV system impedance is modeled to observe the distortions absorbed from the grid in Section 4.9.

4.6.1 Photovoltaic System

Since converter manufacturers usually do not disclose their filter and controller details, assumptions of the harmonic current injections are made for this study. In the first set of cases in this study, the PV inverter is modeled with reduced characteristic harmonics using the Norton equivalent. The Norton equivalent impedance is set to a very large number so almost no current is absorbed from the grid.

The harmonic current injections are limited to comply the IEEE 1547-2018 standard [10], which defines limits for renewable energy sources. The characteristic harmonics of a two-level PWM inverter described in Section 3.2, up to the 50th-order harmonic, are considered for the PV inverter. It is assumed that the two-level VSC converter is compliant with the standard and it is generating up to 75$[\%]$ of the standard limit in the worst case. The characteristic harmonics are reduced proportionally according to the 23rd harmonic component in Figure 3.6. Due to nonidealities in the grid, the noncharacteristic harmonic components are set to 0.1$[\%]$. The assumed harmonic current injections for the PV inverters are shown in Table 4.6.

Table 4.6: PV current harmonic injection assumptions based on IEEE 1547 [10] limits and characteristic harmonic spectrum

Harmonic Order	IEEE 1547 Limit (I_h/I, %)	Value Used (I_h/I, %)	Harmonic Order	IEEE 1547 Limit (I_h/I, %)	Value Used (I_h/I, %)
2	1	0.1	20 - 22	1.5	0.1
3	4	0.1	23	0.6	0.45
4	2	0.1	24 - 34	0.6	0.1
5	4	0.1	35 - 40	0.3	0.1
6	3	0.1	41	0.3	0.225
7 - 10	4	0.1	42	0.3	0.1
11 - 16	2	0.1	43	0.3	0.225
17 - 18	1.5	0.1	44 - 50	0.3	0.1
19	1.5	0.45			

4.6.2 Electric Vehicle Charger

The current harmonic spectrum of the EV charger uses the characteristic six-pulse harmonics from Figure 3.3. The assumed harmonic current injections for the EV charging stations are shown in Table 4.7, which represent characteristic harmonic current injections without a filter. All of the characteristic harmonics violate the IEEE 519:2014 current distortion limits, so a filter is required.

Table 4.7: Six-pulse characteristic harmonic current injections for EV Chargers without a filter from Figure 3.3 compared with IEEE 519:2014 limits (100<I_{sc}/I_L<1000)

Harmonic Order	Value Used (I_h/I_1, %)	IEEE 519 Limit (Ih/I1, %)	Harmonic Order	Value Used (I_h/I_1, %)	IEEE 519 Limit (Ih/I1, %)
5	20	12	29	3.23	2
7	14.29	12	31	2.86	2
11	9.09	5.5	37	2.70	1
13	7.69	5.5	41	2.44	1
17	5.88	5	43	2.33	1
19	5.26	5	47	2.13	1
23	4.35	2	49	2.04	1
25	3.45	2			

4.7 EV Charger Filter Design

The characteristic six-pulse and twelve-pulse current harmonic injections alone are above the limits for IEEE 519:2014 ($100 < I_{sc}/I_L < 1000$) given in Table 2.3. The filter connection to the grid and charger is shown in Figure 4.2.

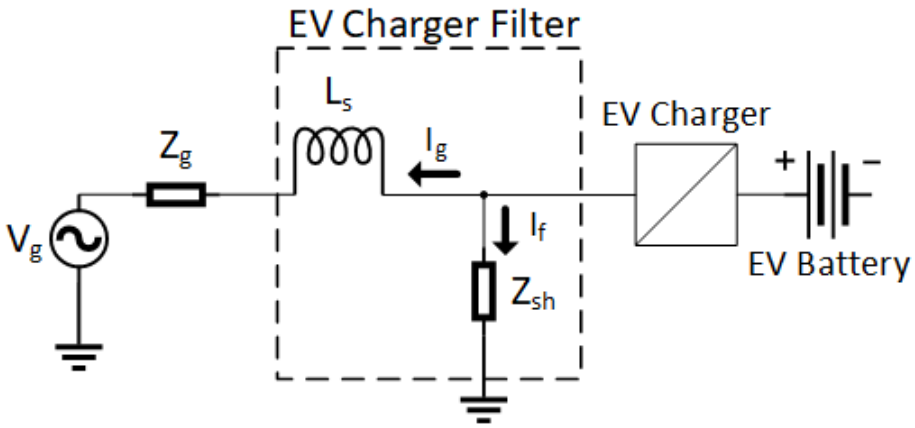

Figure 4.2: EV Charger and Grid Configuration. Z_{sh} represents the single-tuned branches and high-pass shunt filter in parallel, L_s represents the device transformer, Z_g represents the network impedance, and V_g represents the grid voltage at PCC

The filter designed in this section is for a 5 [kVA] EV charger. The first version of harmonic filter designed for the six-pulse rectifier consists of two single-tuned filters, one for the 5th and 7th orders, and one for the 11th and 13th orders. It's parameters are given in Table 4.8. The second variation has individual single-tuned filters for each of those orders, with parameters given in Table 4.9. Both variations have the same high-pass filter in parallel, to reduce the higher-order harmonics, with parameters given in Table 4.10.

Table 4.8: EV Charger Filter: Two Single-tuned Branch Parameters

Harmonic Order	Reactive Power (kVAR)	Resistance (Ω)	Inductance (mH)	Capacitance (uF)	Quality Factor	Rated Current (A)
6	1.8	3.05	8.08	34.84	5	2.6
12	0.9	2.98	3.95	17.79	5	1.3

Table 4.9: EV Charger Filter: Four Single-tuned Branch Parameters

Harmonic Order	Reactive Power (kVAR)	Resistance (Ω)	Inductance (mH)	Capacitance (uF)	Quality Factor	Rated Current (A)
5	1.1	0.60	19.14	21.17	50	1.6
7	0.76	0.61	13.92	14.85	50	1.1
11	0.48	0.60	8.75	9.57	50	0.7
13	0.42	0.60	7.29	8.22	50	0.6

Table 4.10: EV Charger: High-Pass Filter Parameters

Tuned Order	Reactive Power (kVAR)	Quality Factor (QF)	Capacitance (uF)	Inductance (mH)	Resistance Rs (Ω)	Resistance Rp (Ω)
17	2.42	40	41.21	0.85	0	181.76

The single-tuned branches of the filter variations are tuned by setting the rated current to the value measured from the characteristic six-pulse current harmonics. The reactive power generated by the each variations is about 2.7 [kVAR]. The high-pass filter is rated for the measured characteristic currents of the 17th through 50th harmonics.

To meet IEEE 519:2014 standard limits at PCC and match the battery voltage, a 7 [kVA] grid-side transformer with 1.7 [%] impedance is added at the output of the rectifier filter.

The comparison between the impedances of the filter variations and the grid impedance is shown in Figure 4.3. There is a big difference in the impedance of the two filter variations at the low-order characteristic harmonic orders of the six-pulse rectifier (5, 7, 11, and 13). The variation with four single-tuned branches, has a much lower impedance at those frequencies, which can lead to a better harmonic filter.

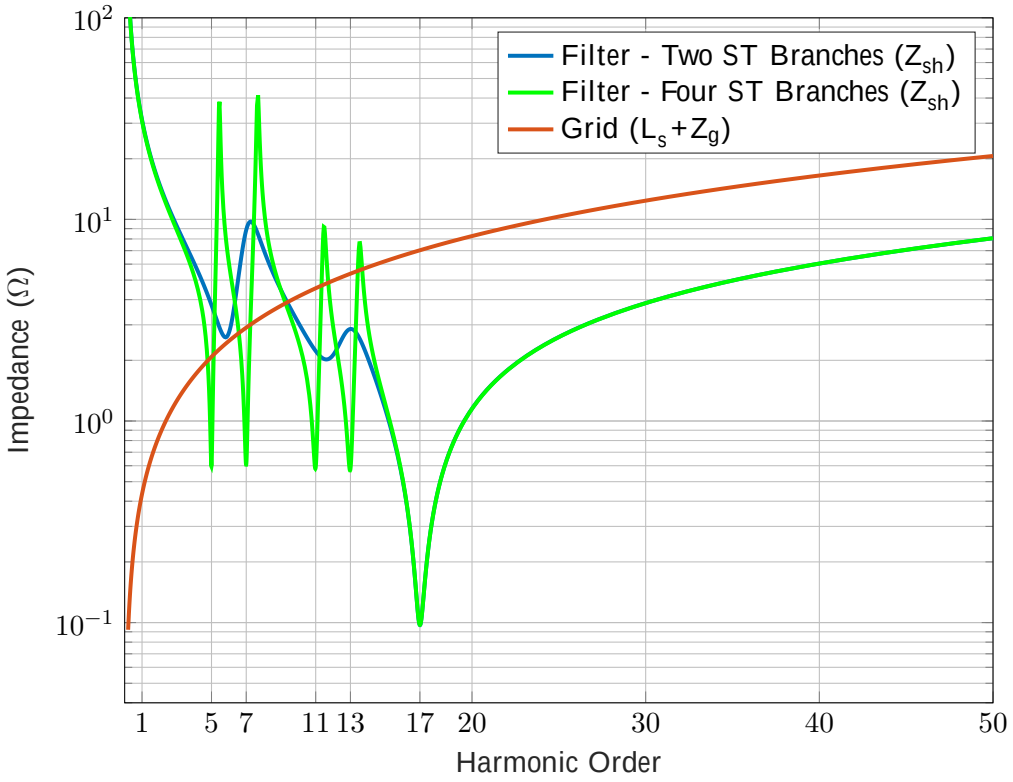

Figure 4.3: Two vs. Four ST Filter comparison with grid impedance from converter view

The comparison using current harmonics is shown in Figure 4.4. Having the individual ST branches for the low-order harmonics greatly improves the current distortion. Therefore, the second filter variation with four ST branches and a HP branch is used in the study.

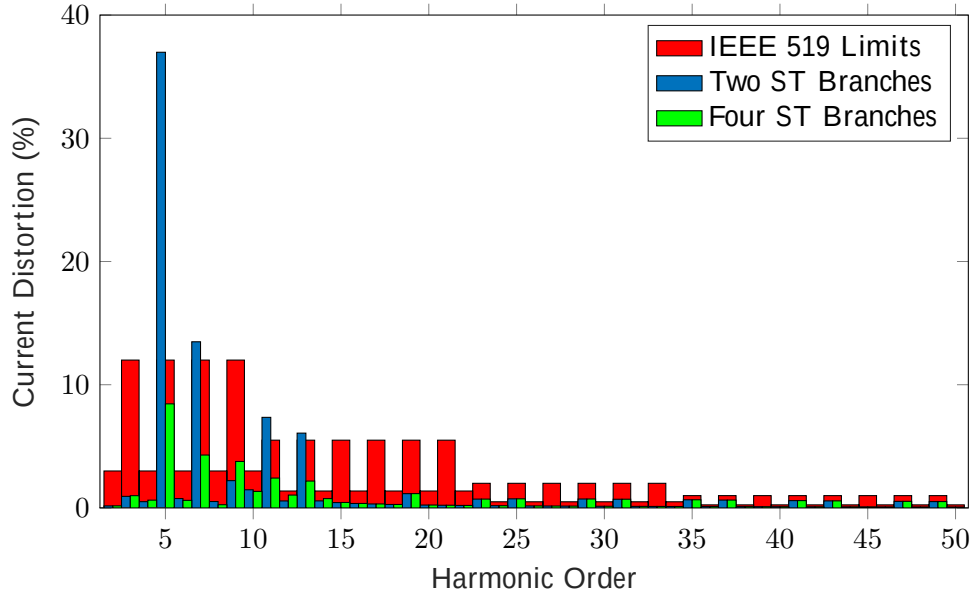

Figure 4.4: Two vs. Four single-tuned filter current harmonics comparison with IEEE 519:2014 ($100 < I_{sc}/I_L < 1000$) limits

The e□ectiveness of the selected filter can be measured by ρ_f from (2.8). This tells the proportion of the current from the nonlinear load that flows to the shunt filter. The impedances are shown in Table 4.11. The filter is absorbing most of the harmonic current distortions at the characteristic harmonic frequencies shown.

Table 4.11: EV Filter E□ciency

Harmonic Order	Filter Impedance (Ω)	Grid Impedance (Ω)	ρ_f	Harmonic Order	Filter Impedance (Ω)	Grid Impedance (Ω)	ρ_f
5	0.6	2.08	0.78	29	4.17	12.10	0.74
7	0.61	2.90	0.83	31	4.71	12.94	0.73
11	0.59	4.56	0.88	35	5.74	14.63	0.72
13	0.58	5.38	0.90	37	6.23	15.48	0.71
17	0.11	7.03	0.98	41	6.72	16.32	0.71
19	0.95	7.88	0.89	43	7.67	18.01	0.70
23	2.40	9.57	0.80	47	8.6	19.70	0.70
25	3.02	10.41	0.77	49	9.06	20.55	0.69

4.8 Cases

There are di□erent cases conducted:

- Base Case - Loads 1-6 from Table 4.4
- Case 1 - Maximum PV System Capacity (270 kW) on Terminal 8
- Case 2 - Unfiltered EV Charger 1 (5 kVA)
- Case 3 - Filtered EV Charger 1 (5 kVA)
- Case 4 - Maximum EV Penetration on Terminal 8
- Case 5 - 270 [kW] PV System and Four 50 [kVA] EV Chargers

Cases 1-5 include the loads from the base case and the extra load(s) mentioned.

4.8.1 Base Case

In the base case, no nonlinear loads are connected to the studied feeder. The loads in the base case are Load 1-6 from Table 4.4. The 500 kVA step-up transformer is 85.9[%] loaded. Table 4.12 shows the measured THD_v and fundamental voltage of each busbar in the feeder.

Table 4.12: Voltage THD_v in the residential feeder in the Base Case

Busbar	THD_v [%]	Voltage (pu)
1	1.22	1
2	1.10	0.97
3	1.11	0.95
4	1.12	0.93
5	1.12	0.92
6	1.12	0.91
7	1.13	0.91
8	1.13	0.91

The voltage distortion graphs on the secondary terminals of the transformer are shown in Figure 4.5. The background harmonics defined in Table 4.2 are the source of these voltage distortions. The background harmonics alone cause a small voltage distortion, but it is about 50[%] of the lowest limits in the IEC 61000-2-2 standard.

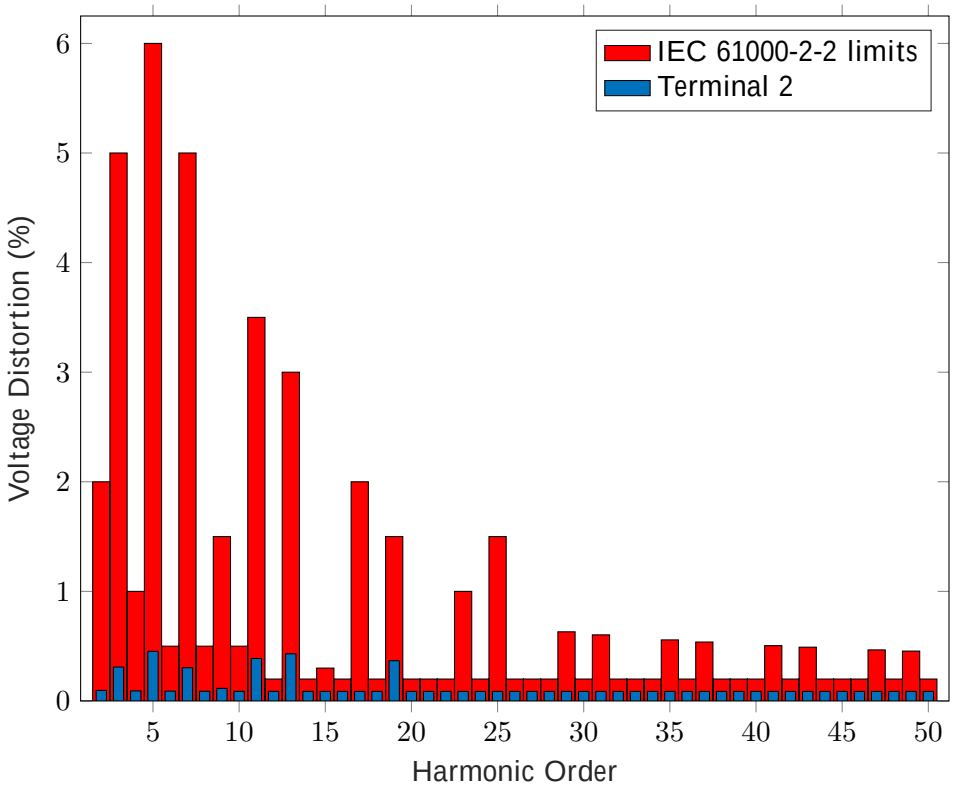

Figure 4.5: Base case harmonic distortion on Terminal 2

Figure 4.6 shows the current harmonic distortion through the transformer. The transformer's largely inductive impedance leads to increased impedance at higher frequencies, and is responsible for the general decreasing trend in current harmonics as frequency increases.

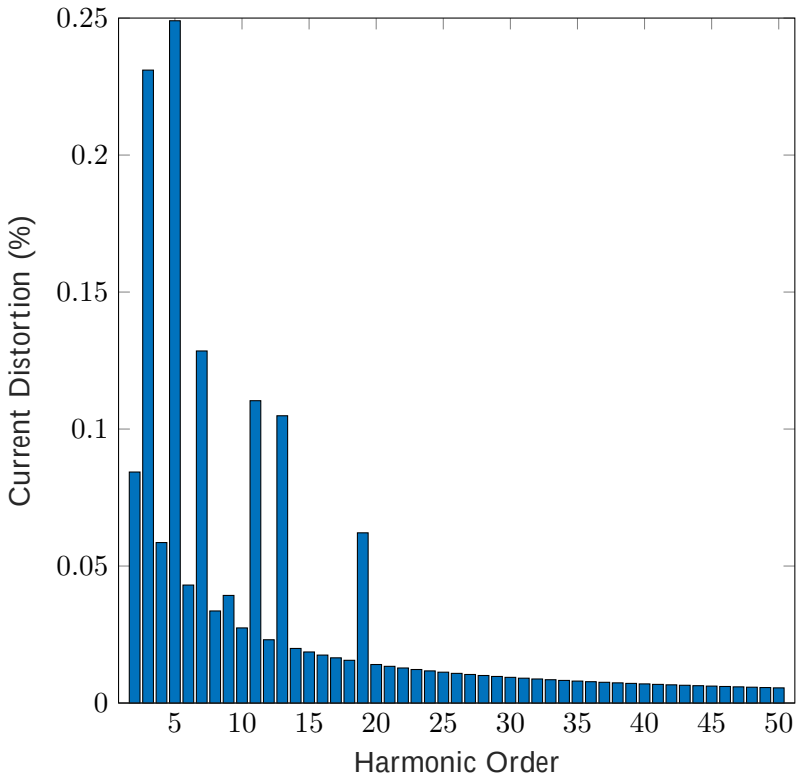

Figure 4.6: Base case current harmonic distortion through the 500 [kVA] distribution transformer from background harmonics

The network impedance is calculated using a frequency sweep on the busbars of the model. The grid impedance on most of the feeder busbars are shown in Figure 4.7. This shows the grid impedance is mostly inductive, increasing impedance with frequency. It represents the impedance from the cables, transformer, and external grid. The grid impedance is lower at the feeder busbars closer to the transformer.

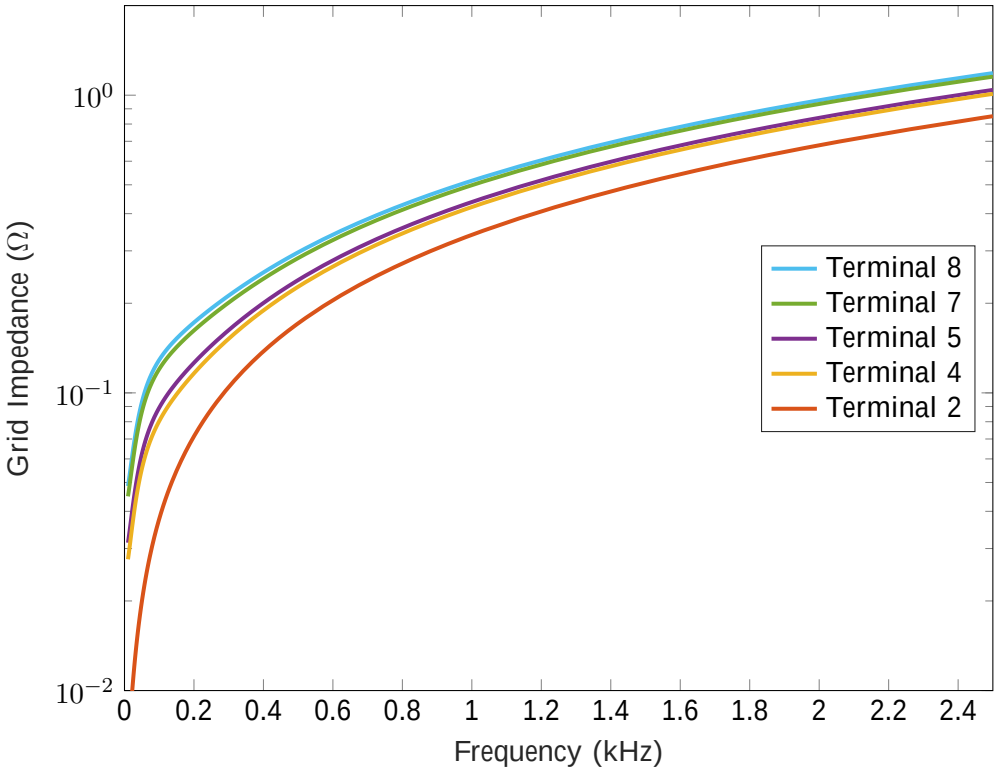

Figure 4.7: Base case grid impedance

The maximum PV penetration can be estimated from the grid impedance in the studied harmonic frequency range. The estimated maximum PV penetration in the grid is calculated at Terminal 8 since it has the highest measured grid impedance. It is calculated based on the limiting harmonic distortion limit, shown in Table 4.13. The maximum estimated PV penetration available at Terminal 8 is about 270 [kW], limited by the 50th harmonic voltage distortion. The 50th order harmonic distortion is from nonidealities, so the characteristic harmonics in this case are not causing the limit violation. This is not a big concern since high-order harmonics can be filtered with a damped filter.

Table 4.13: Maximum Estimated PV Penetration on Terminal 8

Harmonic Order	Network Impedance, Magnitude (Ω)	IEC 61000-2-2 Voltage limit (%)	PV Current Distortion (%)	PV Harmonic Current (mA/kW)	Maximum Estimated PV Penetration (kW)
19	0.4939	1.5	0.45	6.5	1079.9
23	0.5824	1	0.45	6.5	610.5
41	0.9840	0.505	0.225	3.2	364.9
43	1.0288	0.491	0.225	3.2	339.2
50	1.1860	0.2	0.1	1.4	**269.8**

4.8.2 Case 1 - PV System 2 (80[%] and 100[%] PV Capacity - Terminal 8)

This study case observes the effect of adding 80[%] and 100[%] of the maximum estimated PV capacity calculated from Table 4.13. The voltage and THD_v measured at each bus with 100[%] PV capacity (270 [kW]) in the model is shown in Table 4.14. All voltages and THD_s are within the respective limits.

Table 4.14: Voltage THD in the residential feeder with 100% PV Penetration (270 kW) added

Busbar	THD_v [%]	Voltage (pu)
1	1.23	1
2	1.36	0.98
3	1.39	0.98
4	1.44	0.99
5	1.45	0.99
6	1.49	1.01
7	1.51	1.02
8	1.52	1.03

Figure 4.8 compares the voltage distortion between 80[%] and 100[%] of the estimated maximum PV penetration. As predicted in Table 4.13, the IEC 61000-2-2 voltage distortion limits are violated at the 50th harmonic order with 270 [kW] PV penetration at Terminal 8. The high-order harmonics are easier to filter with a damped filter, which would increase the potential PV penetration.

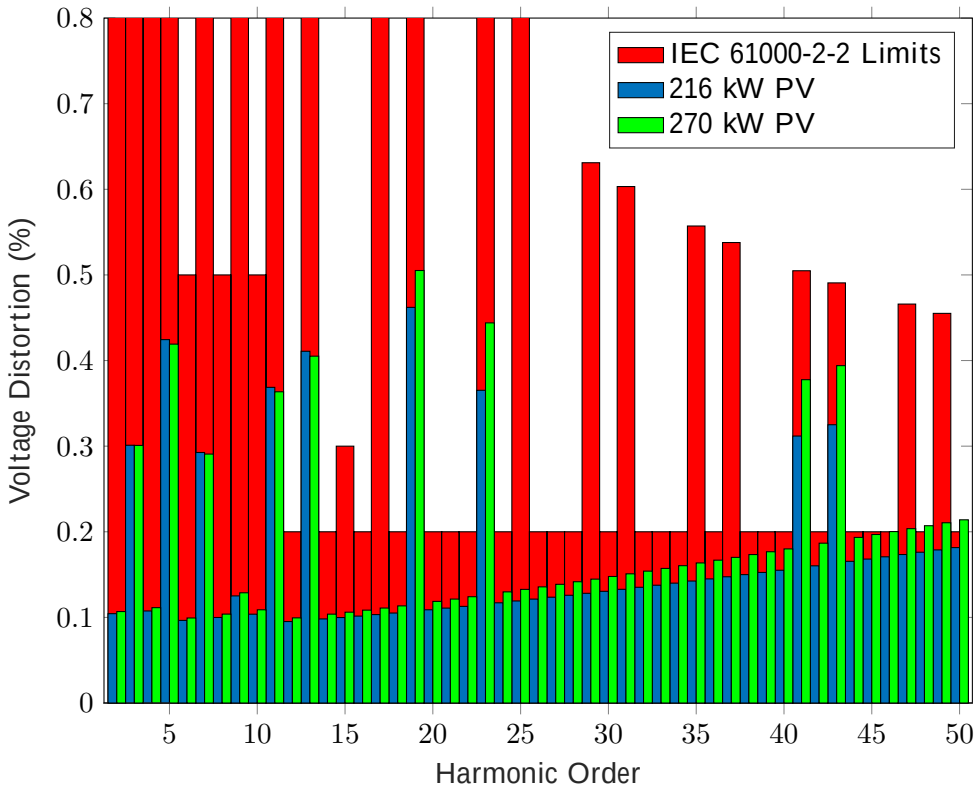

Figure 4.8: Voltage distortion with 80[%] and 100[%] estimated PV capacity based on 270 [kW] limit from Table 4.13. The y axis is limited to 0.8[%] to show the voltage distortion exceeding the IEC 61000-2-2 limits for the high orders.

4.8.3 Cases 2 - 4 - EV Cases

Case 2 - Unfiltered EV Charger 1 (5 [kVA] - Terminal 4)

This case depicts the e□ect of unfiltered Graetz - bridge EV charger harmonics on a low-voltage grid. This shows the harmonic impact and the justification of standards to limit them. Figure 4.9 compares the characteristic six-pulse current distortions to the IEEE 519:2014 limits in Table 2.3 ($100<I_{sc}/I_L<1000$), and shows that they are above the limits for almost all harmonic orders. The TDD is also measured as 30.02$[\%]$, which is above the 12$[\%]$ limit. Adding the filter explained in Section 4.7 is justified.

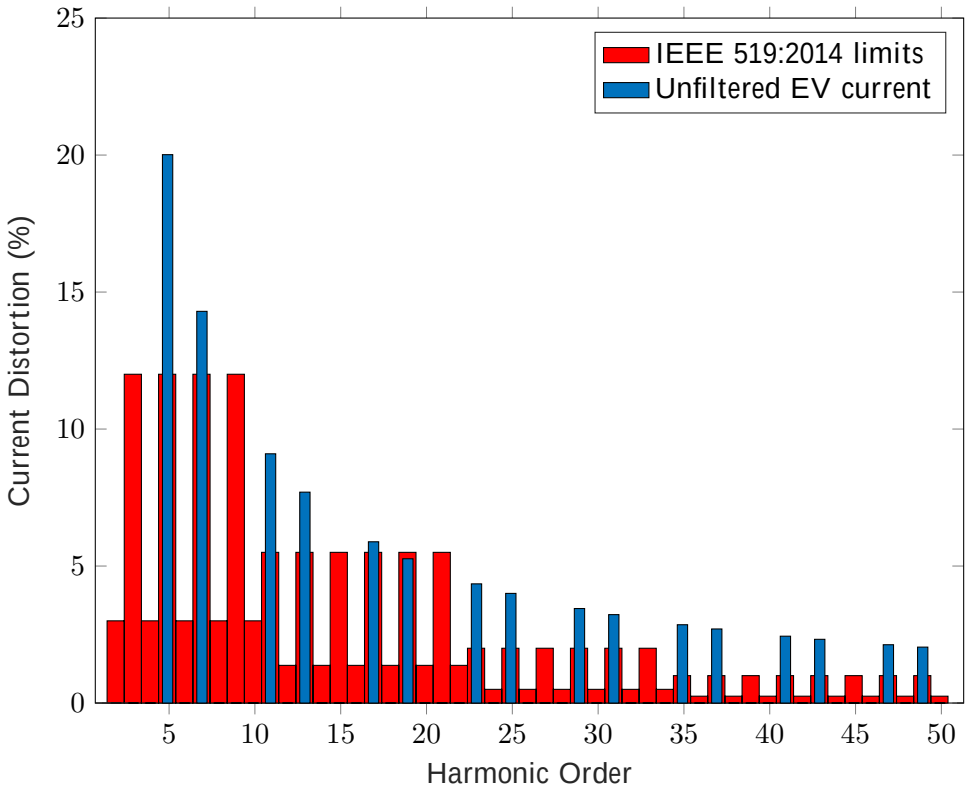

Figure 4.9: Unfiltered EV (5 [kVA]) current harmonic distortion at PCC compared to IEEE 519:2014 limits from Table 2.3 (100<I_{sc}/I_L<1000)

The decaying pattern of harmonic current for the six-pulse converter is observed, as explained in Section 3.1. Since the EV charger has a small output compared to the total feeder load and the grid is sti□, there is almost no change in the voltage harmonics.

Case 3 - Filtered EV Charger 1 (5 [kVA] - Terminal 4)

This case repeats the harmonic studies from previous case but with the designed filter explained in Section 4.6. Figure 4.10 compares filtered EV current harmonics to the IEEE 519:2014 standard (100<I_{sc}/I_L<1000) in Table 2.3. They are all below the limits and several percent lower than in the case without filter. The TDD is measured at 11.25$[\%]$, which is under the 12$[\%]$ limit. Current distortions also appear at more harmonic orders due to current flowing from the grid into the filter. The largest new current distortions can be seen at the ninth and tenth order.

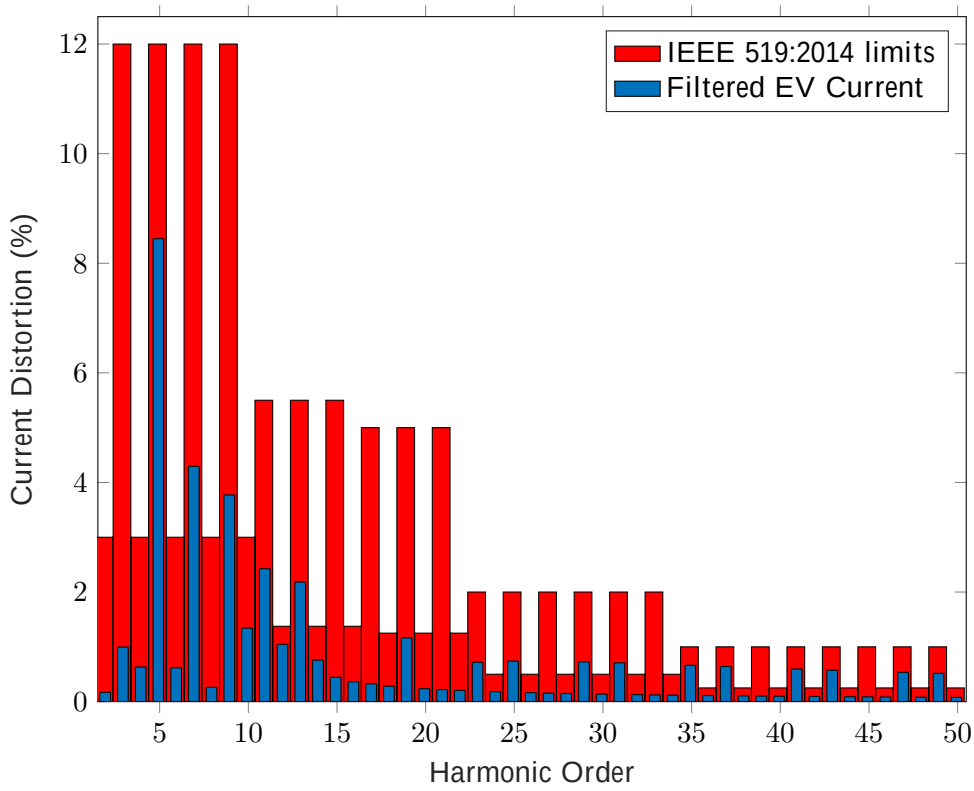

Figure 4.10: 5 [kVA] Filtered EV current harmonic distortion at PCC compared to IEEE 519:2014 standard ($100 < I_{sc}/I_L < 1000$) in Table 2.3

Figure 4.11 shows how the grid impedance measured from PCC changes after adding the EV filter. The local maxima are parallel resonance points and the local minima are series resonance points. The transformer between the grid and EV charger leads to a significant resonance frequency shift for the high-pass filter. This happens because the largely inductive nature of the transformer acts as an inductor between the grid and the shunt filter. This creates a significant parallel resonance near the 9th harmonic order and a series resonance near the 10th order.

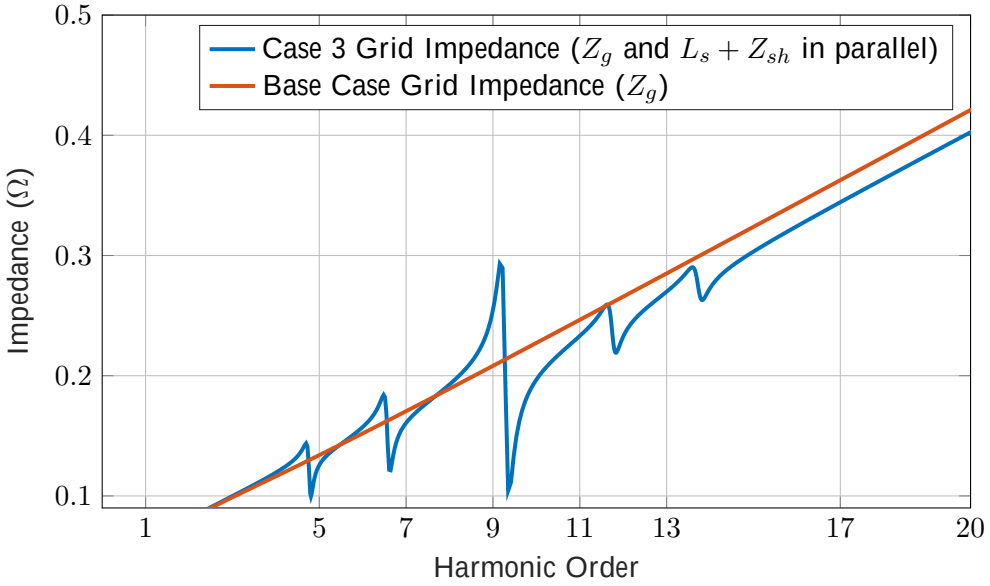

Figure 4.11: Grid Impedance measured from Terminal 4 in Base Case and Case 3

Figure 4.12 compares the voltage harmonic distortion with the to the base case. The difference is small since the EV output is small and the grid is stiff, but some important observations can be noted. The voltage distortion for all harmonics except the 9th order are lower than in the base case. This is because the grid impedance measured at PCC is lower than the base case impedance, as seen in Figure 4.11. The 10th order has an increased impedance due to the parallel resonance from the added filter, which leads to an increase in the harmonic distortion. Even though a filter is added to reduce harmonic distortion, the side effect of the unintended resonance leads to increasing harmonic distortion for one harmonic. This increased voltage distortion could be even larger if more nonlinear loads are added that produce current at the parallel resonance frequency.

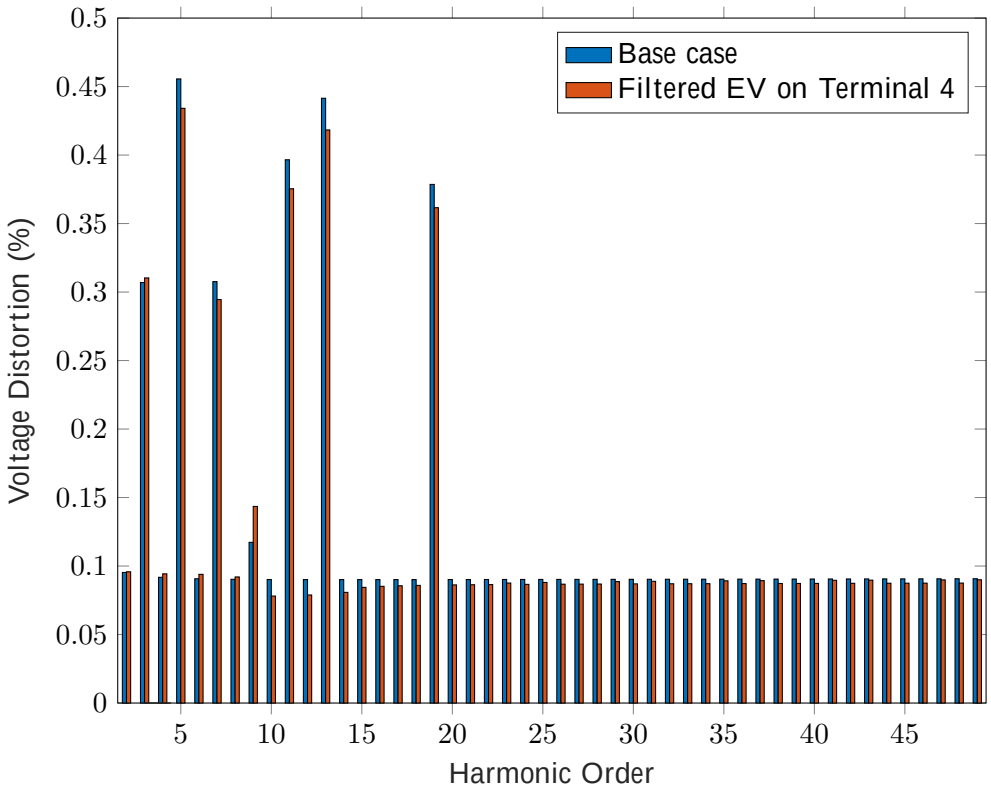

Figure 4.12: Filtered EV (5 [kVA]) harmonic distortion on Terminal 4

Figure 4.13 shows how the EV charger current distortion splits between the filter and grid. It also shows the incoming current distortion from the grid to the filter.

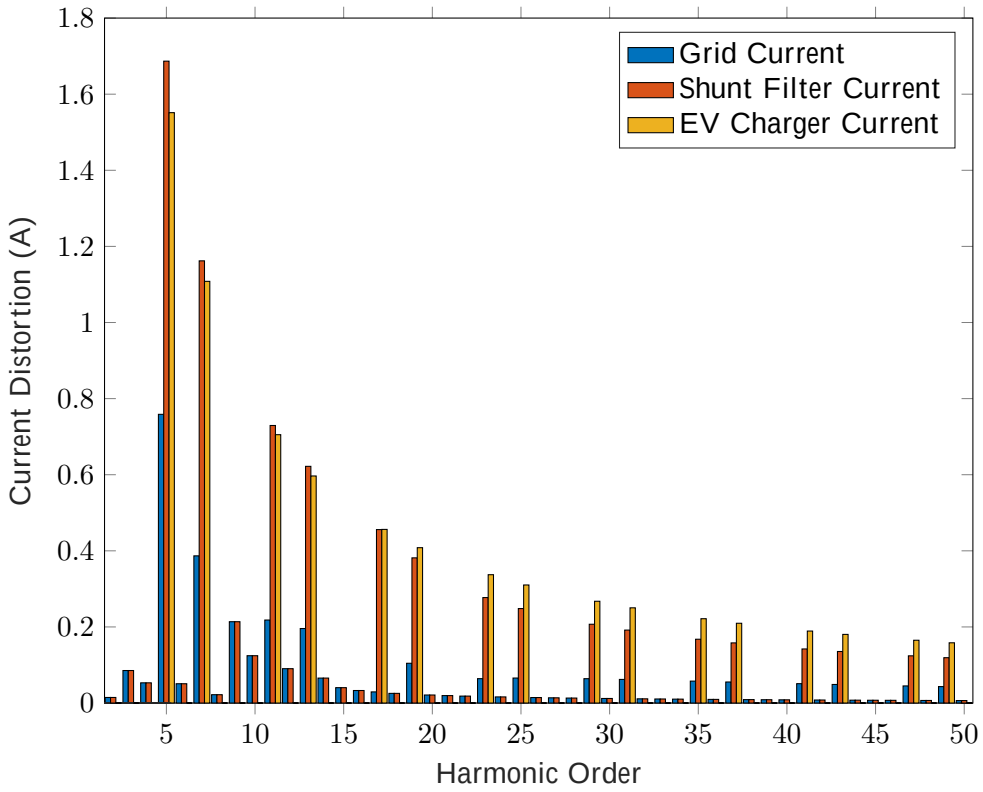

Figure 4.13: EV transformer, EV Charger, and Shunt Filter Current Distortion

4.8.4 Case 4 - Maximum EV on Terminal 8

This section presents a study case where the maximum possible capacity of an EV to install is checked. Terminal 8 is the weakest busbar since it is at the end of the feeder and has the largest measured grid impedance from Figure 4.7. Therefore, the most conservative estimate of EV charger penetration is estimated for this busbar, similar to the study in Section 4.8.2. The EV includes the same filter as in the previous variation.

Adding a 50 $[kVA]$ fast-charging station causes the voltage to drop below the 0.9 [pu] limit to 0.87 $[pu]$ at Terminal 8. To bring voltage back to an acceptable value, the capacity of the charging station has to be decreased. Based on that fact, the maximum EV penetration at Terminal 8 is 19.4 $[kVA]$, keeping the voltage is at the 0.9 $[pu]$ limit.

This shows that the load on the feeder is too large to add high-power EV chargers. The critical parameter limiting the EV penetration in this case is the voltage level at 50 $[Hz]$. The concern of low voltage and further improvement is not included in this project studies. The voltages at the busbars are presented in Table 4.15.

Table 4.15: Voltage at the busbars when EV = 19.4 [kVA] on Terminal 8

Busbar	Voltage (pu)
1	1
2	0.97
3	0.95
4	0.92
5	0.92
6	0.9
7	0.9
8	0.9

4.8.5 Case 5 - 270 [kW] PV System on Terminal 8 and Four 50 [kVA] EV Chargers

This case is conducted to see the impact of both PV system and EV charger on the power quality. Since the barrier to adding more EV chargers in the feeder is fundamental voltage drop, including PV systems allows higher EV penetration. The maximum estimated PV penetration calculated in Section 4.8.1 is used in this case as well. A 50 [kVA] filtered EV charging station is added to Terminals 4, 5, 7, and 8. The THD_v and voltage at each Terminal is given in Table 4.16. The voltage has significantly increased and allowed a larger loading in the feeder.

Table 4.16: Voltage THD_v in the residential feeder with filtered EV and PV

Busbar	THD_v [%]	Voltage (pu)
1	1.20	1
2	1.16	0.99
3	1.19	0.99
4	1.28	0.99
5	1.29	0.98
6	1.33	1.00
7	1.35	1.01
8	1.36	1.02

The harmonic voltage distortion on Terminal 8 is shown in Figure 4.14. The high-order noncharacteristic harmonics are damped in this case from the EV filters. The voltage distortion is now near the limits at the characteristic EV charger harmonics, namely 49th harmonic.

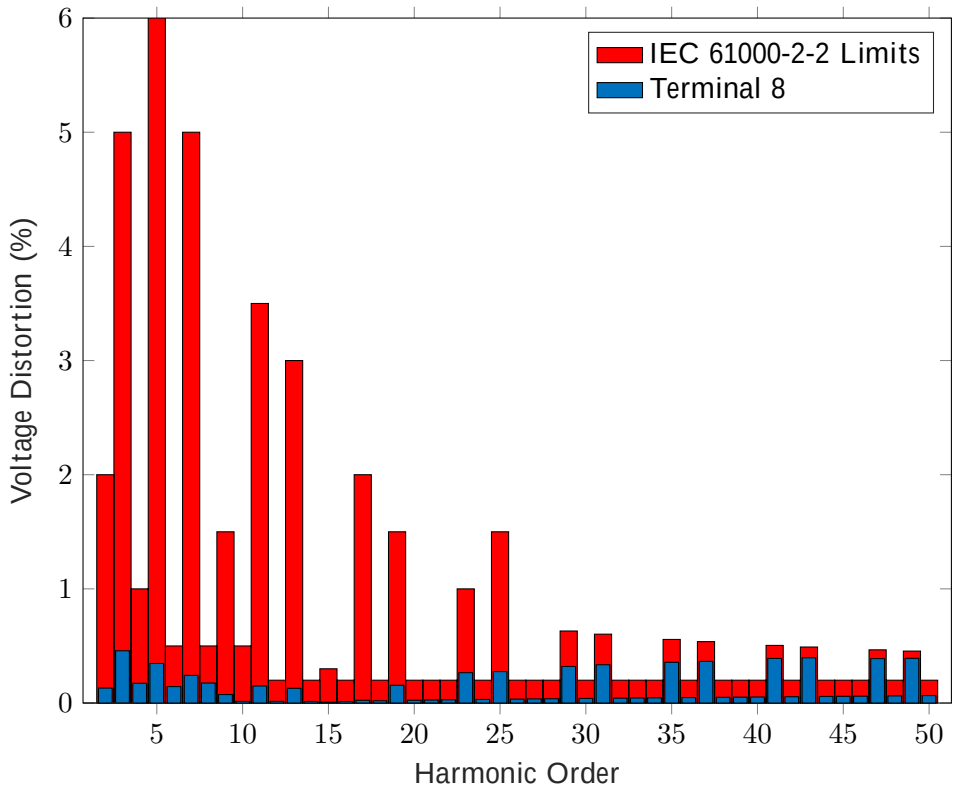

Figure 4.14: Voltage distortion on Terminal 8 with 270 [kW] PV System and four 50 [kVA] EV charging stations

4.9 Modeling Converter as an Equivalent Source

For the sake of this harmonic study, a converter can be modeled as an equivalent source. A power converter can compensate current harmonics. It is an essential function since it can help to limit harmonics. In [29], the modeling of converter through impedance-based analysis is shown. On the grounds of this article a converter is modeled. This model is used for determining a Norton equivalent of the PWM-based PV inverter in this study. Figure 4.15 shows the converter diagram and controllers.

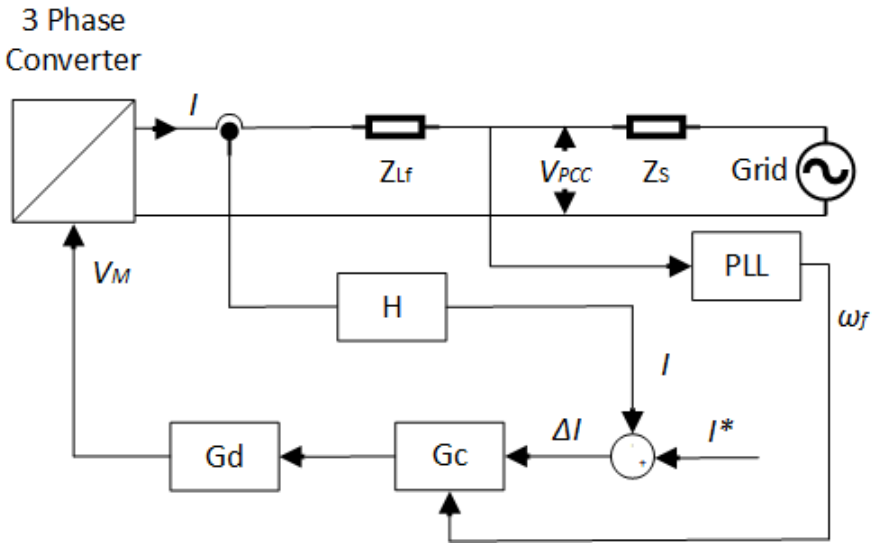

Figure 4.15: 3-phase converter topology and basic control block diagram

Components of the diagram are expressed in the s-domain. The converter has an L-filter, which is shown in the Figure 4.15 as Z_{Lf}, without any extra harmonic filter. The L-filter output admittance describes the converter loop gain term in (4.1), if V_{PCC} = 0 .

$$Y_{Mf} = \frac{1}{Z_{Lf}} \tag{4.1}$$

The admittance between the grid current and Point of Common Coupling is presented in (4.2), if $V_M = 0$.

$$Y_{of} = \frac{1}{Z_{Lf}} \tag{4.2}$$

Controller design is based on the book [30]. Equations 4.3 - 4.6 show derivations of K.

$$\alpha_c = 0.1 \cdot 2\pi \cdot f_{samp} \tag{4.3}$$

$$\alpha_i = 0.05 \cdot \alpha_c \tag{4.4}$$

$$K_p = \alpha_c \cdot L_f \tag{4.5}$$

$$K_i = \alpha_i \cdot L_f \tag{4.6}$$

The proportional resonant controller term is shown in (4.7).

$$G_c = K_p + \frac{K_{i(f)} \cdot s}{s^2 + w_f^2} \tag{4.7}$$

The G_d term represents computation and PWM delay.

$$G_d = e^{-1.5 \cdot s \cdot T_s} \tag{4.8}$$

Eq. (4.9) shows the open-loop gain of the control loop.

$$T_{cf} = G_c \cdot G_d \cdot Y_{Mf} \tag{4.9}$$

The closed loop input admittance is shown in (4.10).

$$Y_{ocf} = \frac{Y_{of}}{1 + T_{cf}} \tag{4.10}$$

The closed loop gain is shown in (4.11). The feedback gain H is assumed to be constant 1.

$$G_{clf} = \frac{T_{cf}}{1 + T_{cf}} \tag{4.11}$$

The output converter current is shown in 4.12.

$$I = G_{clf} \cdot I^* - Y_{ocf} \cdot V_{PCC} \tag{4.12}$$

One of the harmonic compensation methods is to increase the gain of current controller at particular harmonic frequency. The phase-locked loop (PLL) could a□ect the compensation performance because of angle tracking error in the distorted grid voltage [29], but it is not considered in this study. The voltage harmonics emitted by converter appear only in positive sequence, and so the harmonic load flow is computed for positive sequence only, which means the calculation for the harmonic orders being naturally in the negative sequence will be performed with the positive sequence impedance. The values needed to do the calculations are depicted in the Table 4.17.

Table 4.17: Converter parameters

Power rating [kW]	270
Switching frequency [Hz]	1050
Sampling frequency [Hz]	2100
V_{rms} [V]	400
Grid frequency [Hz]	50
L_f [mH]	0.189
R_f [mΩ]	5.9
K_p	0.2489
K_i	0.0124

It is known that converters not only generate distortions to the grid, but also absorb some of them. The comparison with Case 5 is done to see how these two approaches of modeling a converter di□er. To investigate that performance, a 270 [kW] PV converter connected to Terminal 8 is modeled with frequency-dependent impedance and voltage harmonics. Figure 4.16 presents PV converter equivalent impedance from 2nd to 50th harmonic. Fundamental component is enormous, so it is neglected in the figure. Figure 4.17 presents impedance's phase in degrees.

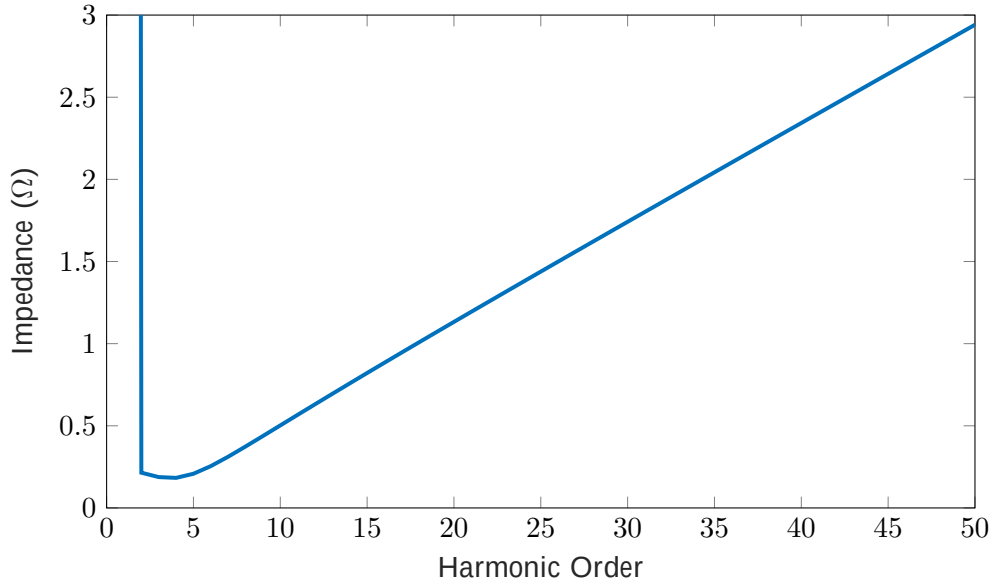

Figure 4.16: 270 [kW] 2-level PV Inverter Impedance Magnitude

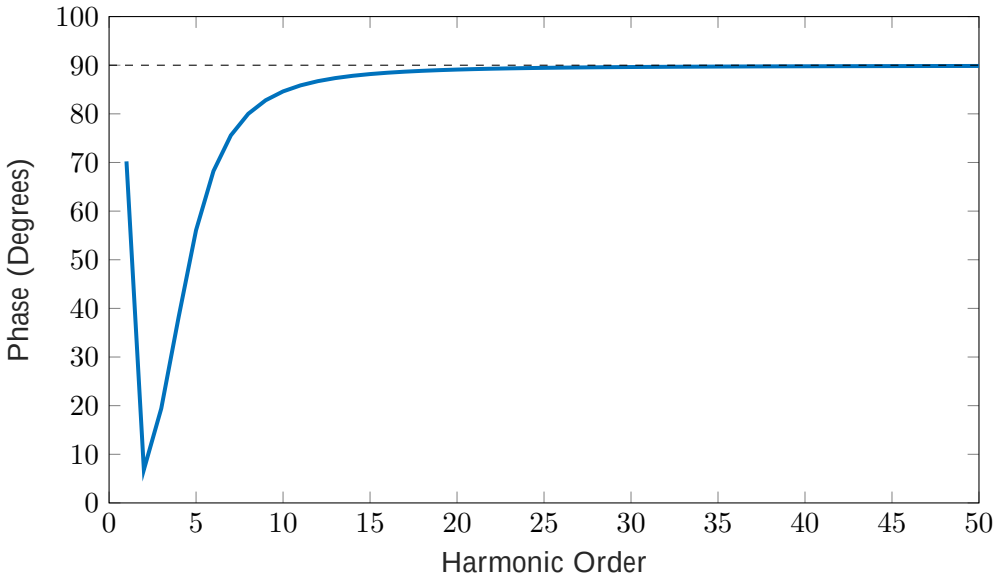

Figure 4.17: 270 [kW] 2-level PV Inverter Impedance Phase

Table 4.18 shows values of resistance and inductance for each harmonic order in absolute units.

Table 4.18: Resistance and Inductance

Harmonic Order	R [Ω]	L [mH]	Harmonic Order	R [Ω]	L [mH]
1	35852383552	3,17461E+11	26	0,013028652	0,183554518
2	0,213078241	0,040620112	27	0,012525962	0,183913596
3	0,177189037	0,066281526	28	0,012074387	0,184236162
4	0,143757177	0,090168781	29	0,01166728	0,184526964
5	0,11610435	0,109923953	30	0,011299028	0,184790011
6	0,094407552	0,125423316	31	0,010964872	0,185028702
7	0,077702974	0,137356134	32	0,010660757	0,185245935
8	0,064864096	0,146527386	33	0,010383207	0,185444193
9	0,054929943	0,153623636	34	0,010129233	0,18562561
10	0,047161846	0,159172578	35	0,009896252	0,185792031
11	0,041014179	0,163563992	36	0,009682024	0,185945056
12	0,036089031	0,167082124	37	0,0094846	0,186086079
13	0,032096223	0,169934261	38	0,009302273	0,186216317
14	0,028822799	0,172272525	39	0,00913355	0,186336838
15	0,026110996	0,17420961	40	0,008977115	0,186448581
16	0,023842674	0,175829909	41	0,008831808	0,186552375
17	0,021928361	0,177197332	42	0,008696602	0,186648955
18	0,020299539	0,178360824	43	0,008570586	0,18673897
19	0,018903159	0,179358278	44	0,008452947	0,186823001
20	0,017697726	0,180219336	45	0,008342961	0,186901565
21	0,016650456	0,180967416	46	0,008239981	0,186975124
22	0,01573521	0,181621188	47	0,008143426	0,187044095
23	0,014930964	0,182195672	48	0,008052774	0,187108848
24	0,014220667	0,182703046	49	0,007967555	0,187169722
25	0,013590386	0,183153264	50	0,007887344	0,187227018

Figure 4.18 highlights the current distortion difference when compared to the previous PV modeling in Section 4.6.1. It can be observed that the magnitude is higher for characteristic harmonics, causing power quality problems and polluting the grid, which means the converter would need extra filter modeling to meet standards. Figure 4.19 depicts voltage harmonic distortion emitted by converter, previously shown in Figure 3.6.

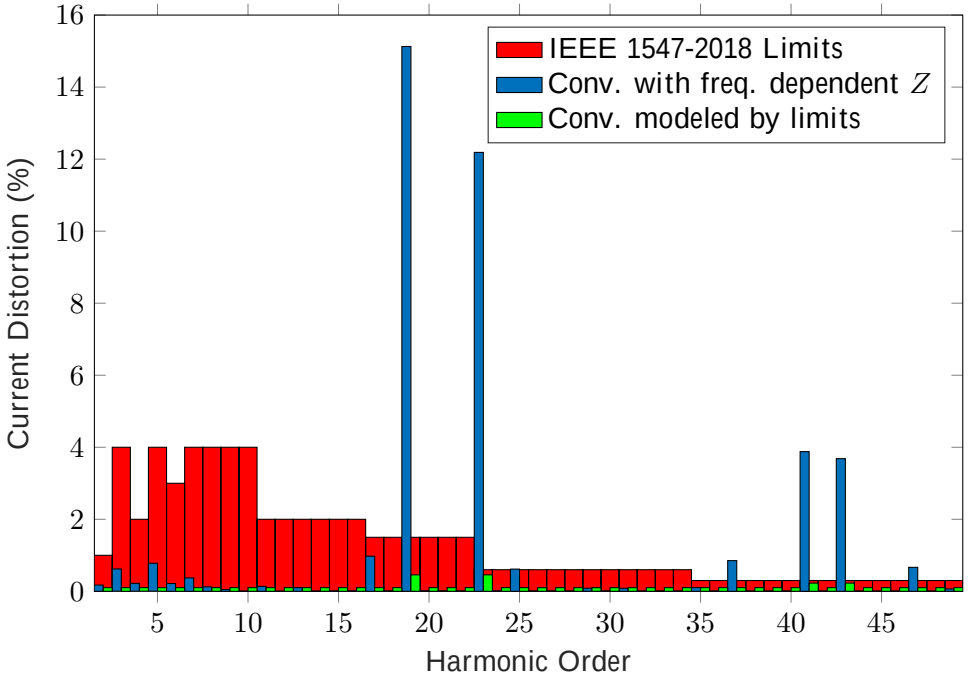

Figure 4.18: Current harmonic distortion for two cases: PV inverter with frequency dependent impedance defined in Table 4.18 versus PV inverter modeled in previous cases

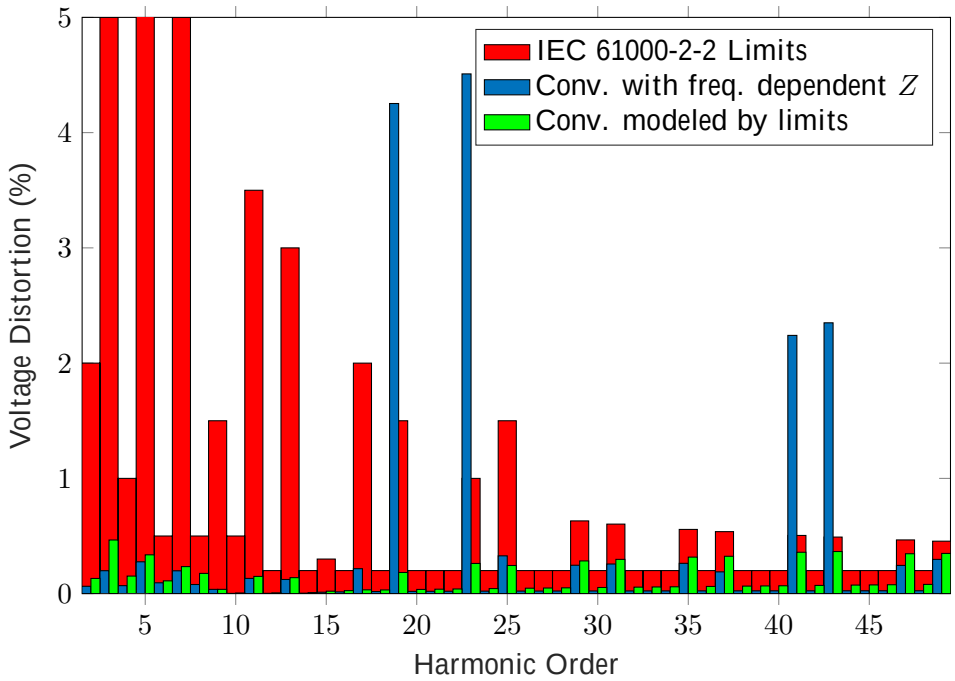

Figure 4.19: Voltage harmonic distortion for two cases: PV inverter with frequency dependent impedance defined in Table 4.18 versus PV inverter modeled in previous cases

4.10 Summary

In this chapter, the test grid, assumed harmonic injections, and study cases are defined and analyzed. Filter design is performed for the EV charger to comply with the IEEE

519:2014 current harmonic limits. The variation with four single-tuned filters is chosen over the variation with two single-tuned filters based on the improved current distortion. The addition of the EV filter lowers its current distortion and improves the voltage harmonics at the PCC. It also absorbs distortion in the grid that was not created by the EV. An unintended consequence of adding the filter is the addition of resonance points near the low-order harmonics, with the most significant one at the 9th harmonic order. The maximum EV charger capacity in the feeder was low since the voltage drop at the end of the feeder could not be supported.

The maximum PV capacity is estimated to be 270 [kW] in the feeder based on the grid impedance measured at the end of the feeder. This estimate considers a PV system that injects current harmonics below the IEEE 1547-2018 limits without a filter. The barrier to adding more PV is the harmonic voltage distortion at high orders. The PV capacity can be increased with an added high-pass filter.

Combining the maximum PV capacity and filtered EV improves the voltage at the end of the feeder and allows more EV chargers to be added. The EV filter also absorbs some of the high-order harmonic from the PV system. The limiting factor then becomes the harmonic distortion from the EV charger characteristic harmonics at the 49th order.

Di□erent converter harmonic injection method is proposed - Equivalent source. It is more precise to the real application, because it considers filter and controller transfer functions. Equivalent source modeling highlights the need of filter, since characteristic harmonics are beyond the standard limits.

Conclusions and Future Work

5

The scope of this thesis is to investigate the impact of different penetration levels of PVs and EVs on the harmonic power quality in a distribution grid. The residential feeder is based on a CIGRE benchmark grid for renewable energy studies with some modification explained in Chapter 4. Due to the fact that this project is focused on harmonic studies, standards such as IEC 61000-2-2, IEEE 519:2014 and IEEE 1547-2018 are utilized. The results are split up into several cases.

The project includes two types of converter: six-pulse full-bridge converter and 2-level voltage source converter. Each converter has its own characteristic harmonics, which are injected and distort the grid more as their penetration level increases.Each network has a limited capability of renewable energy sources and non-linear loads. In this project, the maximum PV capacity is limited by higher order harmonics from nonidealities when assuming current injections based IEEE 1547-2018 limits. Through the unfiltered EV case, it is proved that converters without a filter can pollute the grid more than the standards allow. Moreover, installing and connecting large loads like EV chargers could not only lead to harmonic issues but also significant voltage drops at fundamental frequency. Case 4 shows that the critical factor limiting the case could be voltage level below the limits.

Solutions for the harmonic distortions are implemented through filtering. The voltage harmonic distortion in the feeder changes depending on how the filter alters the grid impedance. The filters added to the EV chargers lower the harmonic distortion in the grid and allow more loads. PV inverters could be filtered for example with damped filter, to increase the maximum PV capacity. Single-tuned filters work more efficiently when designed for one particular frequency instead of covering a range of frequencies. On the other hand, covering more than one frequency might be cheaper in a real application.

The important consequence of adding resonances in the grid due to filters is explored. Parallel resonance tends to increase the harmonic distortion and grid impedance. Lowering the grid impedance through series resonance can decrease the harmonic distortion. As new nonlinear loads and filters are added, the changes to resonance frequencies in the grid can contribute to greater harmonic distortions.

The method of determining the equivalent model of a PV inverter is also described and tested. The purpose of using the equivalent PV model in this study is to observe a more realistic performance. The power quality issue is highlighted for characteristic harmonics, which can be damped by an additional filter. It is shown that the equivalent model is more accurate and looks much different from making assumptions based on standards, because it

considers many variables e.g. switching frequency and controller transfer function. When considering the future layout of distribution grids with many more distributed energy sources, all of the mentioned aspects should be taken into consideration.

Future Work

Due to the complexity of the topic the project is limited to some extent and could be extended much further depends on the will. Some aspects to investigate in the future are proposed:

1. Other types of converters could be utilized including e.g. 12-pulse bridge converter, multi-level voltage source converter, modular multilevel converter (MMC)
2. Unbalanced harmonic load flow with single-phase nonlinear loads
3. Additional feeders and zones from the benchmark grid
4. EV batteries supportive role to the grid
5. The study could be performed in Electromagnetic Transients (EMT) simulation in order to consider di□erent charging stages of a battery and PV output fluctuations due to the weather conditions

Appendix 6

Table 6.1: Cables details

From	To	Conductor ID	Length [m]
Terminal 2	Junction 1	UG1	35
Junction 1	Terminal 3	UG1	35
Terminal 3	Junction 2	UG3	30
Terminal 3	Junction 3	UG1	35
Junction 3	Junction 4	UG3	135
Junction 3	Terminal 4	UG1	70
Terminal 4	Terminal 5	UG1	30
Terminal 4	Junction 5	UG1	70
Junction 5	Terminal 6	UG1	35
Terminal 6	Junction 6	UG3	30
Terminal 6	Terminal 7	UG1	35
Terminal 7	Terminal 8	UG1	30

Bibliography

[1] European Commission. COM(2014) 15 final: A policy framework for climate and energy in the period from 2020 to 2030. pages 1–18, 2014.

[2] Murat Erhan Balci, Shady H. E. Abdel Aleem, and Ahmed Zobaa. *Power System Harmonics - Analysis, E ects and Mitigation Solutions for Power Quality Improvement*. InTechOpen, 2018.

[3] IEEE recommended practice and requirements for harmonic control in electric power systems. *IEEE Std 519-2014 (Revision of IEEE Std 519-1992)*, pages 1–29, 6 2014.

[4] *Electromagnetic compatibility (EMC) - Part 3-2: Limits – Limits for harmonic current emissions (equipment input current = 16 A per phase).* DS/EN ; 61000-3-2. Dansk Standard, Charlottenlund, 3rd edition, 2014.

[5] J. Desai, Pradeep Dadhich, and P. Bhatt. Investigations on harmonics in smart distribution grid with solar pv integration. *Technology and Economics of Smart Grids and Sustainable Energy*, 1(1):1,11, 2016-12.

[6] M Sidrach-de Cardona and J Carretero. Analysis of the current total harmonic distortion for di erent single-phase inverters for grid-connected pv-systems. *Solar Energy Materials And Solar Cells*, 87(1-4):529,540, 2005-05.

[7] *Voltage characteristics of electricity supplied by public electricity networks.* DS/EN ; 50160. Dansk Standard, Charlottenlund, 4th edition, 2010.

[8] Chinthaka Seneviratne and C Ozansoy. Frequency response due to a large generator loss with the increasing penetration of wind/PV generation: A literature review. 57:659–668, 2016.

[9] Bhim Singh. *Power quality problems and mitigation techniques*. Wiley, Chichester, England.

[10] *IEEE Std 1547-2018 (Revision of IEEE Std 1547-2003): IEEE Standard for Interconnection and Interoperability of Distributed Energy Resources with Associated Electric Power Systems Interfaces*. IEEE, 2018.

[11] G Chicco, J Schlabbach, and A.F Spertino. Characterisation and assessment of the harmonic emission of grid-connected photovoltaic systems. In *2005 IEEE Russia Power Tech*, pages 1,7. IEEE, 2005-06.

[12] Zhao Xiangyang and Liu Shiyang. A research of harmonics for multiple pv inverters in grid-connected. In *2012 Asia-Pacific Power and Energy Engineering Conference*, pages 1,4. IEEE, 2012-03.

[13] F. Barakou, M. H. J. Bollen, S. Mousavi-Gargari, O. Lennerhag, P. A. A. F. Wouters, and E. F. Steennis. Impact of load modeling on the harmonic impedance seen from the transmission network. In *2016 17th International Conference on Harmonics and Quality of Power (ICHQP)*, pages 283–288, Oct 2016.

[14] O. Ceaki, G. Seritan, R. Vatu, and M. Mancasi. Analysis of power quality improvement in smart grids. In *2017 10th International Symposium on Advanced Topics in Electrical Engineering, ATEE 2017*. Institute of Electrical and Electronics Engineers Inc., 2017-04-19.

[15] C. Jiang, R. Torquato, D. Salles, and W. Xu. Method to assess the power-quality impact of plug-in electric vehicles. *IEEE Transactions on Power Delivery*, 29(2):958–965, April 2014.

[16] A. Pan and T. Chen. Electric vehicle development in china and its power quality challenges to distribution grid. In *CIRED Workshop 2016*, pages 1–4, June 2016.

[17] D. Fernandez, S. Pedraza, D. Celeita, and G. Ramos. Electrical vehicles impact analysis for distribution systems with thd and load profile study. In *2015 IEEE Workshop on Power Electronics and Power Quality Applications (PEPQA)*, pages 1–6, June 2015.

[18] D. R. Pinto, V. T. Arioli, G. R. T. Hax, F. K. Taniguchi, R. Torquato, W. W. Teixeira, and P. L. Eduardo Jr. Field investigation of the power quality impact of electric vehicles in secondary residential systems. In *2018 18th International Conference on Harmonics and Quality of Power (ICHQP)*, pages 1–6, May 2018.

[19] J. C. Das. *Power system analysis : short-circuit load flow and harmonics /*. Power engineering ; 33. CRC Press, Boca Raton, 2nd edition.

[20] *Power system harmonics*. J. Wiley & Sons, West Sussex, England ;, 2nd edition.

[21] M. Hojabri, M. Hojabri, and A. Toudeshki. Third-order passive filter improvement for renewable energy systems to meet ieee 519-1992 standard limits. In *2015 IEEE Conference on Energy Conversion (CENCON)*, pages 199–204, Oct 2015.

[22] D. Grahame. Holmes. *Pulse width modulation for power converters : principles and practice*. IEEE series on power engineering. John Wiley, Hoboken, NJ.

[23] Energinet technical regulation 3.2.1 for power plants up to and including 11 kw. pages 1–51, 6 2016.

[24] DIgSILENT GmbH. *PowerFactory 2020 User Manual*. `https://www.digsilent.de/en/powerfactory-download.html?folder=files%2Fdownloads%2Fprivate%2F10_PowerFactory%2F00_PowerFactory_2020%2F60_User+Manual#navigation7105`, 2019. Visited 05-03-2020.

[25] CIGRE. Benchmark systems for network integration of renewable and distributed energy resources. pages 54–66, 2014.

[26] National Grid. Generator Self Build Enduring Regime Harmonic Assessment Process Flow. Technical report.

[27] Jeddah cables company. Low voltage cables. page 20, 2014.

[28] Nvent. *What is Soil Resistivity and How Does it A ect Grounding?* https://blog.nvent.com/erico/erico-what-is-soil-resistivity-and-how-does-it-affect-grounding/, 2019. Visited 15-04-2020.

[29] J. Kwon, X. Wang, C. L. Bak, and F. Blaabjerg. Modeling and grid impedance variation analysis of parallel connected grid connected inverter based on impedance based harmonic analysis. In *IECON 2014 - 40th Annual Conference of the IEEE Industrial Electronics Society*, pages 4967–4973, 2014.

[30] Hans-Peter Nee Sta an Norrga Remus Teodorescu Kamran Sharifabadi, Lennart Harnefors. *Design, Control, and Application of Modular Multilevel Converters for HVDC Transmission Systems*. Wiley.